

Pair Production in a Color Glass Condensate Background

Master's Thesis, 16.6.2023

Author:

PATRICIA GIMENO ESTIVILL

Supervisor:

TUOMAS LAPPI



UNIVERSITY OF JYVÄSKYLÄ
DEPARTMENT OF PHYSICS

© 2023 Patricia Gimeno Estivill

This publication is copyrighted. You may download, display and print it for Your own personal use. Commercial use is prohibited. Julkaisu on tekijänoikeussäännösten alainen. Teosta voi lukea ja tulostaa henkilökohtaista käyttöä varten. Käyttö kaupallisiin tarkoituksiin on kielletty.

Abstract

Gimeno Estivill, Patricia

Pair Production in Color Glass Condensate Background

Master's thesis

Department of Physics, University of Jyväskylä, 2023, 57 pages.

At high energy, the density of gluons in hadrons strongly increases until saturation, leading to a state of condensed gluon matter. In high energy collisions, the interaction of partons with this dense gluonic state is represented through Wilson Lines in the Color Glass Condensate theory, which describes the properties of small- x gluons in the saturated regime. In relativistic proton-nucleus collisions, the proton can be treated as a dilute system where a gluon fluctuates into a quark-antiquark pair. In this thesis, the interaction of these gluon and quark/antiquark partons with the condensed gluon matter in the nucleus is studied. Concretely, the quark pair production amplitude is calculated using the dilute-dense approximation in the covariant and in the Light Cone Perturbation theories. Firstly, in covariant theory the proton and nucleus are described as classical fields originating from color sources. As another approach, the initial gluon and the final quark-antiquark states are expanded in terms of the Fock state basis in Light Cone Perturbation Theory. A comparison of the two results is made at the end.

Keywords: Color Glass Condensate, gluon saturation, classical color fields, Wilson Lines, light cone quantization

Preface

Throughout the eight months that I have been developing this thesis, there has not been any moment where intellectual enrichment was not present. I would like to thank Professor Tuomas Lappi for putting the color in my master's thesis.

Jyväskylä June 16, 2023

Patricia Gimeno Estivill

Contents

Abstract	3
Preface	5
1 Introduction	9
2 The Color Glass Condensate	11
2.1 Light cone coordinates	11
2.2 Parton densities of a proton at high energies	12
2.3 Dilute-dense approximation	14
3 Pair Production in Covariant Theory	17
3.1 Classical color fields from Yang-Mills equations	17
3.2 Quark-antiquark production amplitude	21
3.2.1 Regular terms	22
3.2.2 Singular term	31
3.2.3 Complete time-ordered amplitude	33
4 Pair production in Light Cone Perturbation Theory	35
4.1 Perturbative Fock state expansion	35
4.2 Initial and final Fock states in mixed space	38
4.3 Light cone wave function	40
4.4 Pair production amplitude	41
5 Comparison of the results	47
6 Conclusions	53
References	54

1 Introduction

Hadrons are made of quarks that are bound together by the exchange of gluons. Strong interactions between these partons and their properties are described by the Quantum Chromodynamics (QCD) field theory. QCD attributes the forces among partons (quarks and gluons) to the color charge that they carry and it predicts that gluons exchanged between quarks can temporally fluctuate into quark-antiquarks pairs that can produce further gluon emissions and splittings [1]. A prominent feature of the quark and gluon content in hadrons at the high energy (or small- x) regime is the strong increase of the gluon distribution over the quark distribution, which was experimentally observed at HERA electron-proton collider [2]. This growth in the gluon distribution generates a saturation momentum scale Q_s which measures the strength of the gluon recombination processes. Any process involving momenta smaller than Q_s may be affected by gluon saturation [1].

The Color Glass Condensate (CGC) theory describes the behavior of this saturated gluon matter which appears in high energy scatterings such as Deep Inelastic Scattering (DIS) at HERA, nucleus-nucleus or proton-nucleus collisions at the Large Hadron Collider (LHC), as well as lepton-ion collisions in the future Electron Ion Collider (EIC). This thesis is focused on proton-nucleus collisions where a gluon from the proton splits into a quark-antiquark ($q\bar{q}$) pair. The interaction of these partons (both quarks and gluon) with the gluon condensate in the nucleus is described through Wilson Lines in the Eikonal approximation. The main point of this work is the calculation of the pair production amplitude at lowest order in the strong coupling constant. This calculation is performed in two different theories, separately. In section 3, the $q\bar{q}$ -pair production amplitude is obtained by modelling the partons as classical color fields in covariant theory. In this approach, the valence quarks act as large- x color sources for the classical fields, which can be solved from the Yang-Mills equations of motion [3]. Another approach is considered in section 4, where Light Cone Perturbation Theory (LCPT) is used to expand the initial gluon and final $q\bar{q}$ -states in terms of the Fock state basis and Light Cone Wavefunctions (LCWF). The production amplitude is then calculated from the scattering matrix

element between the initial and final states. Finally, the amplitudes obtained in covariant and LCPT theories are compared in section 5.

2 The Color Glass Condensate

2.1 Light cone coordinates

Throughout this thesis, the high-energy proton-nucleus collision is described using light cone coordinates [4, 5] whose components are defined in terms of an arbitrary 4-vector $v^\mu = (v^0, v^1, v^2, v^3)$ as

$$v^+ = \frac{v^0 + v^3}{\sqrt{2}}, \quad v^- = \frac{v^0 - v^3}{\sqrt{2}}, \quad \mathbf{v}_\perp = (v^1, v^2). \quad (1)$$

The non-zero elements of the metric tensor $g^{\mu\nu}$ are

$$g^{+-} = g^{-+} = 1, \quad g^{11} = g^{22} = -1, \quad (2)$$

which implies that

$$v^+ = g^{+\nu} v_\nu = v_-, \quad v^- = g^{-\nu} v_\nu = v_+. \quad (3)$$

The light-like variable $x^+ = \frac{1}{\sqrt{2}}(t+z)$ is usually referred to the “time” coordinate¹ and $x^- = \frac{1}{\sqrt{2}}(t-z)$ to the longitudinal “spatial” coordinate.

The scalar product between two vectors is defined as

$$x \cdot p = g_{\mu\nu} x^\mu p^\nu = x^+ p^- + x^- p^+ - \mathbf{x}_\perp \mathbf{p}_\perp, \quad (4)$$

which suggests that p^- should be interpreted as the light cone energy, because time and energy are conjugate variables. Then, p^+ is interpreted as the light cone longitudinal momentum.

Both coordinates are positive definite ($p^\pm > 0$) for particles propagating in the direction of increasing x^+ , while $p^\pm < 0$ for antiparticles moving in the direction of

¹ The x^+ -coordinate should not be interpreted as the usual time $t = x^0$. In covariant theory, one can make a continuous transformation and boost to any coordinate system moving at velocity $v < 0$, where the physics will look the same with a different coordinate time. However, it is not possible to boost to exactly light velocity $v = 0$. For high energy scattering problems one has to define a coordinate “time” that is a light-like variable [6].

decreasing x^- .

2.2 Parton densities of a proton at high energies

Nucleons are made of three valence quarks bound by gluons. However, these quarks can temporarily fluctuate into states that have additional gluons and sea quarks-antiquarks pairs. These fluctuations are short lived, with a lifetime that is inversely proportional to their energy [1].

In DIS experiments, one probes the proton structure with a lepton, which interacts with the proton by exchanging a photon with virtuality Q^2 . This resolution power Q^2 of the probe sets the characteristic time scale of the reaction and only the fluctuations that are longer lived than the resolution in time of the probe can be seen in the process. Hence, to be able to “see” these fluctuations it is necessary to study a high energy nucleon whose internal scales are time dilated by the Lorentz factor [1].

The experimental data on DIS collected at HERA hadron collider [2] allows to determine the parton distribution functions (PDFs), which give the probability to find partons (quarks and gluons) in a hadron as a function of Bjorken- x . This x is the momentum fraction of the parton on which the photon scatters and it is defined as $x \approx Q^2/W^2$, with W^2 the invariant energy squared of the photon-proton system [7]. Therefore, scatterings at high energy (large W^2 at fixed Q^2) corresponds to small values of x .

An interesting phenomenon occurs at small- x , when the density of gluons inside a proton or nucleus strongly increases until *saturation*, outnumbering the valence and sea parton distributions. This trend can be observed in Figure 1 where the gluon PDF denoted by g clearly dominates the structure of the proton over the sea s, c, \bar{u}, \bar{d} and valence u_v, d_v quarks when $x < 0.1$. This dense state of gluon matter inside a proton or nucleus at small- x is referred to as Color Glass Condensate and it plays a major role in interactions at high energy.

Theoretically, the parton content in hadrons can be studied in perturbative QCD theory with evolution equations that allow to determine the PDFs at some point (x, Q^2) if an initial value at (x_0, Q_0^2) is known [7]. Figure 2 illustrates different evolution equations whose region of validity depends on the momentum scale Q^2 . At high x , the DGLAP evolution equation can be applied to describe a “dilute” hadron or nucleus while the linear BFKL equation [8, 9] predicts the growth of gluon

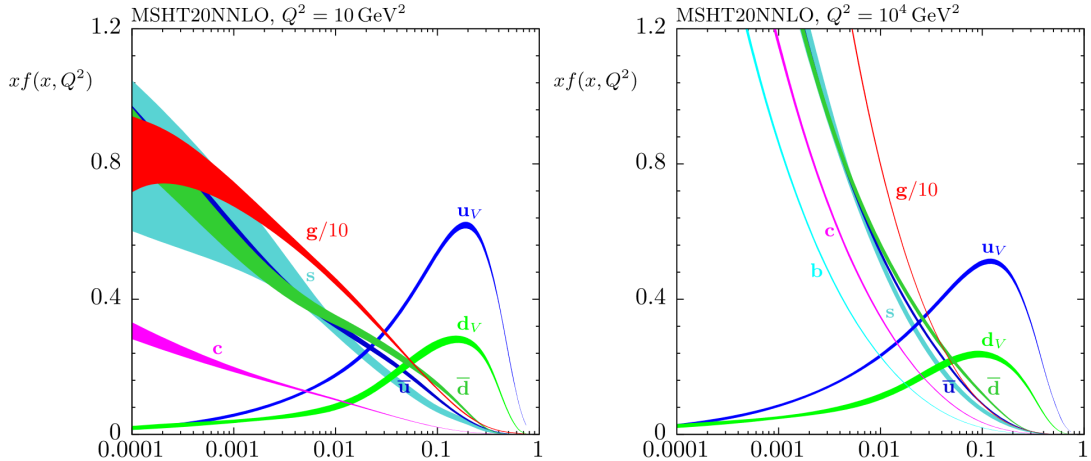


Figure 1. The bands are x times the parton distribution functions of the valence quarks $f = u_v, d_v$, sea quarks $f = \bar{u}, \bar{d}, s, c, b$, and gluons $f = g$, as functions of Bjorken x for fixed scales $Q^2 = 10 \text{ GeV}^2$ (left) and $Q^2 = 10^4 \text{ GeV}^2$ (right). The uncertainties are represented by the bands. Note that the gluon PDF xg is scaled by a factor 1/10. Figure from NNLO MSHT20 global analysis [2].

distribution towards small x .

Although there is no strict bound on the number density of gluons in QCD, scattering cross sections cannot grow faster than $\ln^2 s$ with s the centre of mass energy squared, which is known as the Froissart-Martin bound [10]. This limit in the cross section leads to a limit in the gluon density and therefore, the BFKL equation which predicts a growth in the number of partons as $N \sim (1/x)^\lambda$, with $\lambda > 0$, is not valid at high energy [7]. In this region, it is necessary to consider the recombination of partons ($gg \rightarrow g$) on top of the splitting ($g \rightarrow gg$), which restricts the growth of the gluon density and leads to saturation [1, 11–13]. This transition until saturation is described by the non-linear BK and JIMWLK evolution equations at $Q_s^2 \gg \Lambda_{QCD}^2$, with $\Lambda_{QCD} \approx 200 - 300 \text{ MeV}$ the fundamental scale of QCD [14]. The saturation scale Q_s which characterize the onset of saturation effects induced by the medium grows with decreasing x and increasing mass number of a nucleus A as [14]

$$Q_s^2(x, A) \sim A^{1/3} x^{-\lambda}, \quad (5)$$

with $\lambda \approx 0.2 \dots 0.3$. The power $A^{1/3}$ comes from the radius of the nucleus $R \sim A^{1/3}$ and the λ parameter is obtained from DIS measurements.

Since the running of the strong-coupling $\alpha_s(Q_s)$ is controlled by the saturation

scale Q_s , high energy processes can be described using weak coupling techniques ($\alpha_s(Q_s) \ll 1$) as in perturbation theory.

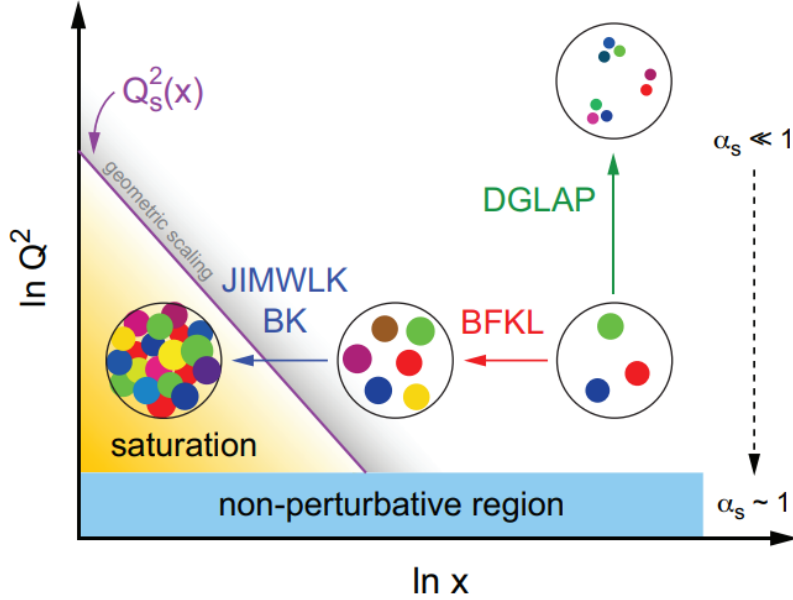


Figure 2. In the perturbative region ($Q^2 \gg \Lambda_{QCD}^2$), the saturation scale Q_s separates the dilute region, where few partons (colored balls) compose the hadron, from the saturation region, where the number of gluons increases. Different evolution equations are used to describe the partonic content depending on the momentum scale Q^2 of the process. Figure from [7].

2.3 Dilute-dense approximation

The kinematic notation for the proton-nucleus scattering is

$$p(p_p) + A(p_A) \rightarrow q(q)\bar{q}(p) + X . \quad (6)$$

As it is shown in Figure 3, the proton moving in the $(+z)$ -direction is defined with momentum $p_p = (p_p^+, 0^-, 0_\perp)$ while the nucleus moving in the $(-z)$ -direction is defined with momentum $p_A = (0^+, p_A^-, 0_\perp)$.

In this collision, the nucleus is approximated as a dense system in the saturation region while the proton is considered to be a dilute system. In the latter, a valence quark emits a gluon with momentum $k_1 = (x_p p_p^+, 0, \mathbf{k}_{1\perp})$ which can fluctuate into a massive quark and antiquark with momentum q and p , respectively. Then, these

partons eikonally interact with the Color Glass Condensate in the nucleus. In the eikonal approximation, the partons do not deviate their trajectory during the interaction, which is represented by a path ordered exponential known as Wilson Line [12, 14].

In the following section 3, the pair production amplitude is calculated in Lorenz/covariant gauge ($\partial_\mu A^\mu = 0$) and in section 4, the probability amplitude describing the same process is calculated in light cone gauge ($A^+ = 0$).

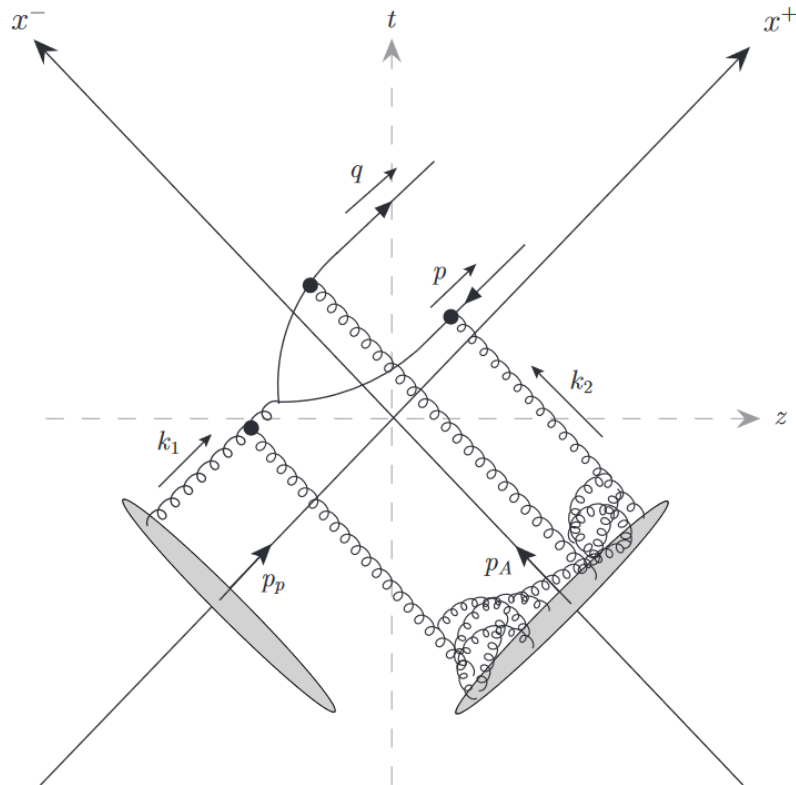


Figure 3. Relativistic p-A collision and quark pair production in light cone coordinates. Both nucleus and proton appear as two dimensional thin sheets due to the Lorentz contraction at relativistic energies. The Wilson lines are illustrated as black dots and represent the multiple scatterings of the corresponding parton off the saturated gluonic region in the nucleus.

3 Pair Production in Covariant Theory

3.1 Classical color fields from Yang-Mills equations

In the CGC effective field theory, the proton-nucleus scattering is described as a collision between two classical fields created by random color sources which represent the valence partons with small momentum (large- x) in each projectile [14, 15]. As a result of Lorentz time dilatation, these color sources are static over the timescale of the collision and treated as a shockwave due to Lorentz contraction [14].

The classical fields are obtained by solving the Yang-Mills equations coupled to a color current [3]

$$[D_\mu, F^{\mu\nu}] = J^\nu, \quad (7)$$

where the field tensor $F^{\mu\nu}$ is defined as

$$F^{\mu\nu,a} = \partial^\mu A^{\nu,a} - \partial^\nu A^{\mu,a} + gf^{abc} A^{\mu,b} A^{\nu,c}. \quad (8)$$

The covariant derivative D_μ is

$$D_\mu = \partial_\mu - igA_\mu^a T^a, \quad (9)$$

where T^a are the generator matrices of the adjoint $SU(N_c)$ algebra. The color current J^ν of the two valence sources is [16]

$$J^{\nu,a} = g\delta^{\nu+}\delta(x^-)\rho_p^a(\mathbf{x}_\perp) + g\delta^{\nu-}\delta(x^+)\rho_A^a(\mathbf{x}_\perp), \quad (10)$$

where the Eikonal sources ρ_p and ρ_A are Lorentz contracted to delta functions $\delta(x^\pm)$ due to the relativistic velocities and independent of the light cone time x^\pm , reflecting their staticity during the time scale of the collision [6].

In Lorenz gauge $\partial_\mu A^\mu = 0$, the classical field separately created by ρ_p in the proton and ρ_A in the nucleus before the collision can be analytically solved to leading

order in the color sources from eq. (7). The results in coordinate space are [16]

$$A_p^\mu(x) = -g\delta^{\mu+}\delta(x^-)\frac{1}{\nabla_\perp^2}\rho_p(\mathbf{x}_\perp), \quad (11)$$

$$A_A^\mu(x) = -g\delta^{\mu-}\delta(x^+)\frac{1}{\nabla_\perp^2}\rho_A(\mathbf{x}_\perp), \quad (12)$$

and their Fourier transform in momentum space results in

$$A_p^\mu(l) = 2\pi g\delta^{\mu+}\delta(l^-)\frac{\rho_p(\mathbf{l}_\perp)}{l_\perp^2}, \quad (13)$$

$$A_A^\mu(l) = 2\pi g\delta^{\mu-}\delta(l^+)\frac{\rho_A(\mathbf{l}_\perp)}{l_\perp^2}. \quad (14)$$

However, the color orientation of the parton in the proton can change after the collision, that is, the color density of the proton can undergo a local rotation in the non-abelian gauge theory of $SU(N_c)$, produced by its interaction with the CGC in the nucleus,

$$e^{i\alpha^a(x)t^a}\rho_a e^{-i\alpha^a(x)t^a} \rightarrow \rho'_a. \quad (15)$$

This implies that higher order corrections in the current in eq. (10) are needed to guarantee its covariant conservation, which is expressed as

$$[D_\nu, J^\nu] = 0. \quad (16)$$

In this way, the total gauge field A^μ emerges from the interaction of the proton source with the gauge field of the nucleus A_A^μ during the collision. Then, the quark pair production can be calculated in the presence of these classical fields without the partonic description of point-like particles.

The analytical solution of eqs. (7) and (16) has been rigorously derived in [3]. This correction, denoted as A^μ , contains singular terms, which are proportional to a $\delta(x^+)$ -function in coordinate space, and regular terms (see section 3.5 of [3]). Thus, this total gauge field is decomposed as

$$A^\mu(l) = A_{\text{reg}}^\mu(l) + A_{\text{sing}}^\mu(l). \quad (17)$$

The regular term A_{reg}^μ is

$$A_{\text{reg}}^\mu(l) = A_p^\mu(l) + \frac{ig}{l^2 + il^+\epsilon} \int \frac{d^2\mathbf{k}_{1\perp}}{(2\pi)^2} \left\{ C_U^\mu(l, \mathbf{k}_{1\perp}) [U_A(\mathbf{k}_{2\perp}) - (2\pi)^2 \delta(\mathbf{k}_{2\perp})] \right. \\ \left. + C_{V, \text{reg}}^\mu(l) [V(\mathbf{k}_{2\perp}) - (2\pi)^2 \delta(\mathbf{k}_{2\perp})] \right\} \frac{\rho_p(\mathbf{k}_{1\perp})}{k_{1\perp}^2}, \quad (18)$$

where $A_{\text{reg}}^{\mu,a}(l) = A_{\text{reg}}^\mu(l) T^a$.

The regular field in eq. (18) is linear in the proton source ρ_p . This is consistent with the analytical description of a dilute-dense collision, where all the expressions expanded in the small parameter ρ_p are truncated to first order. It can also be seen that eq. (18) is expressed as the Fourier transform in eq. (13) of the proton gauge field plus a term that contains the off-shell gluon propagator with momentum l . This second term is originated from the interaction of a gluon with momentum $\mathbf{k}_{1\perp}$ with the CGC in the nucleus, with momentum $\mathbf{k}_{2\perp} \equiv \mathbf{l}_\perp - \mathbf{k}_{1\perp}$. The 4-vectors C_U^μ and $C_{V, \text{reg}}^\mu$ in eq. (18) gather the momentum dependence of the integral and their components are

$$C_U^+(l, \mathbf{k}_{1\perp}) \equiv -\frac{\mathbf{k}_{1\perp}^2}{l^- + i\epsilon}, \quad C_U^-(l, \mathbf{k}_{1\perp}) \equiv \frac{\mathbf{k}_{2\perp}^2 - l_\perp^2}{l^+}, \quad C_U^i(l, \mathbf{k}_{1\perp}) \equiv -2k_1^i, \quad (19)$$

$$C_{V, \text{reg}}^+(l) \equiv 2l^+, \quad C_{V, \text{reg}}^-(l) \equiv 2l^- - \frac{l^2}{l^+}, \quad C_{V, \text{reg}}^i(l) \equiv 2l^i. \quad (20)$$

The U and V terms in eq. (18) are the Fourier transforms of Wilson lines in the adjoint representation of $SU(N)$,

$$U_A(\mathbf{x}_\perp) = \mathcal{P}_+ \exp \left(ig \int_{-\infty}^{+\infty} dz^+ A_A^-(z^+, \mathbf{x}_\perp) \cdot T \right), \quad (21)$$

$$V(\mathbf{x}_\perp) = \mathcal{P}_+ \exp \left(i \frac{g}{2} \int_{-\infty}^{+\infty} dz^+ A_A^-(z^+, \mathbf{x}_\perp) \cdot T \right), \quad (22)$$

where \mathcal{P}_+ is the path-ordering operator along the z^+ -axis. The above exponentials contain the A_A^- gauge field of the nucleus (12) next to the group generators T . As it is discussed in section 2.2 in [3], the nucleus field in eq. (12) is not modified by any correction to higher orders in ρ_A .

The path ordered exponential in eq. (21) sums all powers of gA^- which represents all the scatterings of a particle propagating through the target along the z^+ -axis at a fixed transverse coordinate \mathbf{x}_\perp . Since the generator T belongs to the adjoint

representation, the eikonal particle is a gluon. If the particle is a quark, the Wilson line is denoted by U_F and contains the generator t in the fundamental representation. The propagation of an eikonal antiquark is expressed with the conjugate Wilson line U_F^\dagger . Therefore, this phase acquired by the particle is the result of its interaction with the CGC. The unusual Wilson line V with a factor of $1/2$ in eq. (22) is obtained during the calculation of gluon production in the Lorenz gauge [3], but it does not appear in other gauge calculations, e.g. in [17]. Thus, it is expected that the final quark pair production amplitude does not depend on it.

The relationship between $C_{V,reg}^\mu$ and the vector C_V^μ is [3]

$$C_V^\mu = C_{V,reg}^\mu(l) - \delta^{\mu-} \frac{l^2}{l^+}. \quad (23)$$

It is possible to see that the singular field appears from the second term in eq. (23), where the l^2 term cancels the $1/l^2$ pole in eq. (18) and thus, it is the only term that survives in the limit $l^- \rightarrow \infty$. Therefore, the singular field is

$$A_{\text{sing}}^-(l) = -\frac{ig}{l^+} \int \frac{d^2 \mathbf{k}_{1\perp}}{(2\pi)^2} [V(\mathbf{k}_{2\perp}) - (2\pi)^2 \delta(\mathbf{k}_{2\perp})] \frac{\rho_p(\mathbf{k}_{1\perp})}{k_{1\perp}^2}. \quad (24)$$

In contrast with the regular field expression in eq. (18), eq. (24) does not include the field of the proton alone $A_p^\mu(l)$ since its minus component is zero. The integration over l^- in eq. (24) leads to a $\delta(x^+)$ -function which imposes the gluon production within the nucleus. The Fourier transform of this singular field is

$$A_{\text{sing}}^-(x) = \frac{ig^2}{2} (A_A^-(x) \cdot T) V(x^+, -\infty; \mathbf{x}_\perp) \theta(x^-) \frac{1}{\nabla_\perp^2} \rho_p(\mathbf{x}_\perp), \quad (25)$$

where $V(x^+, -\infty; \mathbf{x}_\perp)$ denotes the incomplete Wilson line

$$V(x^+, -\infty; \mathbf{x}_\perp) = \mathcal{P}_+ \exp \left(i \frac{g}{2} \int_{-\infty}^{x^+} dz^+ A_A^-(z^+, \mathbf{x}_\perp) \cdot T \right). \quad (26)$$

Here x^+ is the point where the gluon splitting is produced inside the nucleus. This longitudinal extension in $V(x)$ (nucleus extension) will be regularized in section (3.2.2). On the other hand, the regular field $A_{\text{reg}}^\mu(l)$ in eq. (18) represents the gluon splitting outside the nucleus.

In this classical field formalism, the quark pair production amplitude in the

Lorenz gauge is calculated in the next section, following [16].

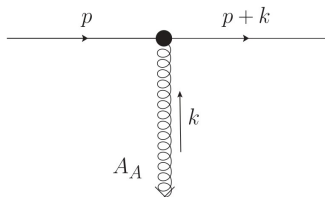
3.2 Quark-antiquark production amplitude

In concordance with the decomposition of the total gauge field A^μ in eq. (17), the calculation of the pair production amplitude is organized in two stages:

1. Regular diagrams, where the $q\bar{q}$ pair is created from the regular field (18) outside the nucleus.
2. Singular diagrams, where the pair is produced from the singular field (25) inside the nucleus.

At the end of the calculation, the two contributions are added to obtain the full covariant amplitude $\mathcal{M}_{\text{cov}} = \mathcal{M}_{\text{reg}} + \mathcal{M}_{\text{sing}}$ in sec. (3.2.3).

To approximate the proton as a dilute system, the Feynman diagrams are drawn with only one insertion of the regular (18) and singular (25) fields on the quark propagator so that the pair production amplitude is calculated to first order in the proton source ρ_p . However, the nuclear field (12) can be added multiple times in the quark and antiquark propagators since it does not change the power counting in the proton source². These multiple interactions are expressed through the following effective vertex³ $\mathcal{T}(k, p)$ symbolized as a single black dot in the diagrams,



$$= 2\pi\delta(k^+)\gamma^+\text{sign}(p^+) \int d^2\mathbf{x}_\perp e^{i\mathbf{k}_\perp \cdot \mathbf{x}_\perp} [U_F^{\text{sign}(p^+)}(\mathbf{x}_\perp) - 1] . \quad (27)$$

Here p is the quark momentum and k is the net momentum transmitted by the multiple gluon “kicks” to the quark. The sign of p^+ depends on whether the gluon insertions are placed in quark ($p^+ > 0$) or antiquark ($p^+ < 0$) lines, where the Wilson Lines (21) in the fundamental representation are respectively denoted by U_F and U_F^\dagger .

The free Feynman propagator for intermediate off-shell quark particles with

² The detailed proof of this statement can be read in [3].

³ The effective vertex is derived in [11, 18] from the Coulomb interaction of a fermion particle with an electromagnetic vector potential created by a nucleus in heavy ion collisions. Although the derivation was performed in Quantum Electrodynamics (QED) to study the e^+e^- pair production in ultra-relativistic nuclear collisions, the analogy with QCD made in this work by replacing the electromagnetic vector potential with the gauge potential leaves the expression of the effective vertex unchanged.

momentum p and mass m is

$$S_0(p) \equiv \frac{i(\not{p} + m)}{p^2 - m^2 + i\epsilon}. \quad (28)$$

Gluon polarization is not considered in the following calculations.

3.2.1 Regular terms

The regular terms in eq. (17) which contribute to the amplitude are represented by the four diagrams in Figure 4.

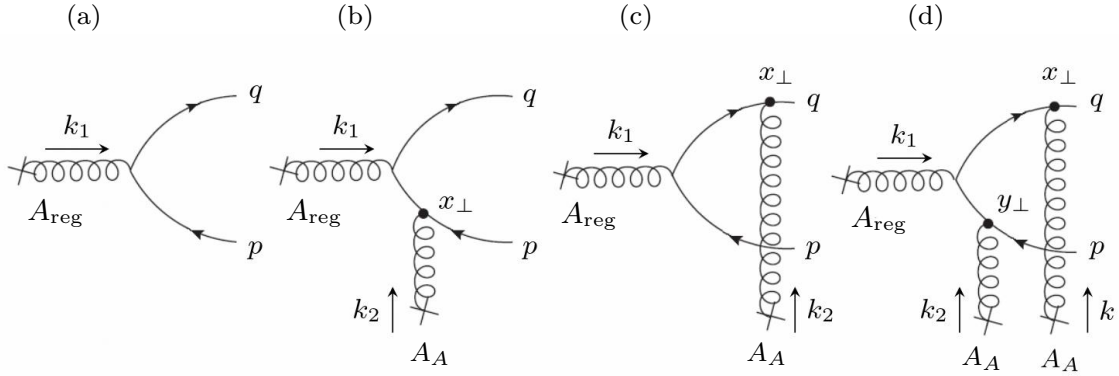


Figure 4. Regular diagrams contributing to the pair production amplitude. The gluon line connected with a cross denotes a classical field insertion. The multiple insertions of the field A_A are represented by a black dot which symbolizes the effective vertex defined in eq. (27).

The contribution of diagram (a) can be written using Feynman rules as

$$\mathcal{M}_{(a)} = \int \frac{d^4 k_1}{(2\pi)^4} \bar{u}(q) [-ig A_{\text{reg}}(k_1) \cdot t] v(p) (2\pi)^4 \delta^4(p + q - k_1). \quad (29)$$

This expression can be integrated over the internal momenta k_1 with the four-dimensional delta function. The regular field $A_{\text{reg}}(k_1)$ has been defined in eq. (18), where now $l = k_1 = p + q$,

$$A_{\text{reg}}^\mu(p + q) = A_p^\mu(p + q) + \frac{ig}{(p + q)^2 + i(p^+ + q^+)\epsilon} \int \frac{d^2 \mathbf{k}_{1\perp}}{(2\pi)^2} \left\{ C_U^\mu(p + q, \mathbf{k}_{1\perp}) \right. \\ \left. \times [U_A(\mathbf{k}_{2\perp}) - (2\pi)^2 \delta(\mathbf{k}_{2\perp})] + C_{V, \text{reg}}^\mu(p + q) [V(\mathbf{k}_{2\perp}) - (2\pi)^2 \delta(\mathbf{k}_{2\perp})] \right\} \frac{\rho_p(\mathbf{k}_{1\perp})}{k_{1\perp}^2}. \quad (30)$$

Since the proton field $A_p^\mu(p+q)$ defined in eq. (13) contains a delta function in the form $\delta(p^- + q^-)$, it needs to be discarded since it would not represent the production of two quarks on-shell, for which $p^- > 0$ and $q^- > 0$. In this diagram (a), this term would mean the production of a pair from the proton alone, which is impossible due to kinematics [16]. Then, the contribution of the first diagram is

$$\begin{aligned} \mathcal{M}_{(a)} = & g^2 \int \frac{d^2 \mathbf{k}_{1\perp}}{(2\pi)^2} \frac{\rho_p(\mathbf{k}_{1\perp})}{k_{1\perp}^2} \int d^2 \mathbf{x}_\perp e^{i(\mathbf{p}_\perp + \mathbf{q}_\perp - \mathbf{k}_{1\perp}) \mathbf{x}_\perp} \\ & \times \left\{ \frac{\bar{u}(q) \not{C}'_U(p+q, \mathbf{k}_{1\perp}) t^b v(p)}{(p+q)^2} [U_A(\mathbf{x}_\perp) - 1]_{ba} - \frac{\bar{u}(q) \gamma^+ t^b v(p)}{p^+ + q^+} [V(\mathbf{x}_\perp) - 1]_{ba} \right\}. \end{aligned} \quad (31)$$

In this expression, the Wilson Lines are Fourier transformed to coordinate space using the momentum conservation $\mathbf{k}_{2\perp} + \mathbf{k}_{1\perp} = \mathbf{p}_\perp + \mathbf{q}_\perp$. Furthermore, the second term in eq. (31) has been obtained using the Dirac equation $\bar{u}(q)(\not{p} + \not{q})v(p) = 0$ to set to zero the first term of the $C_{V,reg}^\mu$ coefficient (20):

$$\begin{aligned} \frac{1}{(p+q)^2} \bar{u}(q) \gamma_\mu C_{V,reg}^\mu(p+q) t^b v(p) &= \\ &= \frac{1}{(p+q)^2} \bar{u}(q) \gamma_\mu \left(2(p^\mu + q^\mu) - \delta^{\mu-} \frac{(p+q)^2}{p^+ + q^+} \right) t^b v(p) \\ &= \frac{1}{(p+q)^2} 2\bar{u}(q) (\not{p} + \not{q}) v(p) t^b - \frac{1}{(p+q)^2} \bar{u}(q) \gamma_\mu \left(\delta^{\mu-} \frac{(p+q)^2}{p^+ + q^+} \right) t^b v(p) \\ &= -\frac{\bar{u}(q) \gamma^+ t^b v(p)}{p^+ + q^+}. \end{aligned} \quad (32)$$

The second diagram in Figure 4 shows the eikonal interaction antiquark-nucleus with the effective vertex $\mathcal{T}(k, -p)$ (27) drawn on the antiquark line. The momentum direction of the intermediate off-shell propagator is defined according to an antiparticle moving backwards in time and thus carrying $-p < 0$ momentum in the direction of the antiquark line. In contrast, the physical/on-shell antiquark has a positive defined

momentum $p > 0$. The amplitude (b) is then written as

$$\begin{aligned}
\mathcal{M}_{(b)} &= \int \frac{d^4 k_1}{(2\pi)^4} \frac{d^4 k_2}{(2\pi)^4} \bar{u}(q) [-ig A_{\text{reg}}(k_1) \cdot t] S_0(-p + k_2) \mathcal{T}(k_2, -p) v(p) \\
&\quad \times (2\pi)^4 \delta^4(p + q - k_1 - k_2) \\
&= - \int \frac{dk_2^+}{2\pi} 2\pi \delta(k_2^+) \\
&\quad \times \int \frac{dk_2^-}{2\pi} [-ig \gamma_\mu A_{\text{reg}}^{\mu a}(p + q - k_2) t^a] S_0(-p + k_2) \\
&\quad \times \int \frac{d^2 \mathbf{k}_{2\perp}}{(2\pi)^2} d^2 \mathbf{x}_\perp e^{i\mathbf{k}_{2\perp} \mathbf{x}_\perp} \bar{u}(q) \gamma^+ [U_F^\dagger(\mathbf{x}_\perp) - 1] v(p) .
\end{aligned} \tag{33}$$

In the second equality, the 4-dimensional delta function has been integrated over k_1 . Also, the effective vertex $\mathcal{T}(k_2, -p)$ (27) has been explicitly written, which brings a minus sign since it is added in the antiquark propagator.

Equation (33) can be further solved by integrating over k_2^+ with the delta function. Then, the k_2^+ -momentum is set to zero, which is compatible with the physical picture of the target nucleus moving in the x^- -direction in the light cone. Subsequently, the k_2^- -integral in eq. (33) is solved by the theorem of residues. The terms which contain the singularities are the intermediate propagator $S_0(-p + k_2)$ (28) and the regular field $A_{\text{reg}}^\mu(p + q - k_2)$ (18). The singularity in the antiquark propagator is

$$\begin{aligned}
(-p + k_2)^2 - m^2 + i\epsilon &= 0 \\
2(-p^+ + k_2^+)(-p^- + k_2^-) - (-\mathbf{p}_\perp + \mathbf{k}_{2\perp})^2 - m^2 + i\epsilon &= 0 \\
2(-p^+)(-p^- + k_2^-) - (-\mathbf{p}_\perp + \mathbf{k}_{2\perp})^2 - m^2 + i\epsilon &= 0 \\
\Rightarrow k_2^- &= p^- + \frac{(-\mathbf{p}_\perp + \mathbf{k}_{2\perp})^2 + m^2}{2(-p^+)} - \frac{i\epsilon}{2(-p^+)} ,
\end{aligned} \tag{34}$$

which is located in the upper half plane of k_2^- . In this calculation, the off-shell propagator is transformed to on-shell, since the isolated pole is located at the square of the particle mass, $p^2 = m^2$.

The first singularity in the regular field $A_{\text{reg}}^\mu(p + q - k_2)$ (18) is found in the

gluon propagator:

$$\begin{aligned}
& \rightarrow (p + q - k_2)^2 + (p^+ + q^+ - k_2^+)i\epsilon = 0 \\
& 2(p^+ + q^+ - k_2^+)(p^- + q^- - k_2^-) - (\mathbf{p}_\perp + \mathbf{q}_\perp - \mathbf{k}_{2\perp})^2 + (p^+ + q^+ - k_2^+)i\epsilon = 0 \\
& (p^- + q^- - k_2^-) = \frac{(\mathbf{p}_\perp + \mathbf{q}_\perp - \mathbf{k}_{2\perp})^2 - (p^+ + q^+)i\epsilon}{2(p^+ + q^+)} \quad (35) \\
& \Rightarrow k_2^- = p^- + q^- - \frac{(\mathbf{p}_\perp + \mathbf{q}_\perp + \mathbf{k}_{2\perp})^2}{2(p^+ + q^+)} + \frac{i\epsilon}{2} .
\end{aligned}$$

The second singularity is carried by the C_U^+ coefficient (19):

$$\begin{aligned}
& \rightarrow p^- + q^- - k_2^- + i\epsilon = 0 \\
& \Rightarrow k_2^- = p^- + q^- + i\epsilon .
\end{aligned} \quad (36)$$

The poles in eqs. (35) and (36) are located above the real axis in the k_2^- plane.

The last calculation cannot be understood as the procedure of putting a propagator on-shell. Instead, the singularity in the C_U^+ component defined in eq. (19) can be explained in the CGC theory: the proton source traveling in the x^+ -direction, can only interact with the classical field of the nucleus at $x^+ > 0$, once it has “seen” the nuclear source, which is moving in the x^- -direction. The Fourier integral of the C_U^+ component is the integral representation of the Heaviside step function, which leads to an interaction between the color sources over the x^+ -axis in the light cone [6].

Since the integrand of eq. (33) is strongly suppressed in the limit $|\vec{k}_2| \rightarrow \infty$, it is possible to apply the residue’s theorem either in the upper or lower semicircle in the k_2^- complex plane. Thus, the k_2^- -integral vanishes when the lower half plane is chosen, since the three poles in eqs. (34), (35) and (36) are located inside the upper semicircle.

Therefore, the only contribution from the regular field $A_{\text{reg}}^\mu(p + q - k_2)$ (18) to the k^- -integral in eq. (33) is the proton field $A_p^\mu(p + q - k_2)$ (13). The latter can be integrated over k^- with the delta function, which imposes $p^- + q^- - k_2^- = 0$. Physically, this result can be interpreted as the creation of the $q\bar{q}$ -pair in the proton and the subsequent interaction of the antiquark with the gluon shock wave of the nucleus.

The final expression of amplitude (b) is written by conveniently replacing the

integration variable over the transverse momentum $\mathbf{k}_{2\perp}$ to $\mathbf{k}_{1\perp} = \mathbf{p}_\perp + \mathbf{q}_\perp - \mathbf{k}_{2\perp}$,

$$\mathcal{M}_{(b)} = +g^2 \int \frac{d^2\mathbf{k}_{1\perp}}{(2\pi)^2} \frac{\rho_p(\mathbf{k}_{1\perp})}{k_1^2} \int d\mathbf{x}_\perp e^{i(\mathbf{p}_\perp + \mathbf{q}_\perp - \mathbf{k}_{1\perp})\mathbf{x}_\perp} \times \frac{\bar{u}(q)\gamma^- t^b (\not{q} - \not{k}_1 + m)\gamma^+ [U_F^\dagger(\mathbf{x}_\perp) - 1]v(p)}{2p^+p^- + (\mathbf{q}_\perp - \mathbf{k}_{1\perp})^2 + m^2}, \quad (37)$$

where the γ^- factor results from the dot product $\gamma_\mu \cdot A_p^+ \rightarrow \gamma^-$. Furthermore, to obtain eq. (37), the propagator $S_0(-p + k_2)$ (28) has been rewritten as

$$\begin{aligned} i \frac{-\not{p} + \not{k}_2 + m}{(p - k_2)^2 - m^2 + i\epsilon} &= i \frac{-\not{p} + \not{k}_2 + m}{2(p^+ - k_2^+)(p^- - k_2^-) - (\mathbf{p}_\perp - \mathbf{k}_{2\perp})^2 - m^2 + i\epsilon} \\ &= i \frac{\not{q} - \not{k}_1 + m}{2(p^+)(-q^-) - (\mathbf{q}_\perp - \mathbf{k}_{1\perp})^2 - m^2 + i\epsilon} \\ &= -i \frac{\not{q} - \not{k}_1 + m}{2p^+q^- + (\mathbf{q}_\perp - \mathbf{k}_{1\perp})^2 + m^2 - i\epsilon}, \end{aligned} \quad (38)$$

where $k_2^+ = 0$, $p^- + q^- = k_2^-$ and $\mathbf{p}_\perp + \mathbf{q}_\perp = \mathbf{k}_{1\perp} + \mathbf{k}_{2\perp}$. The minus sign written in eq. (33) is cancelled by the minus sign obtained in eq. (38), which results in a positive sign in the final amplitude (b) (37).

The contribution of diagram c in Figure (4) is

$$\begin{aligned} \mathcal{M}_{(c)} &= \int \frac{d^4k_1}{(2\pi)^4} \int \frac{d^4k_2}{(2\pi)^4} \bar{u}(q)\mathcal{T}(k_2, q)S_0(q - k_2) [-ig\gamma_\mu A_{\text{reg}}^{\mu a}(k_1)t^a]v(p) \\ &\quad \times (2\pi)^4 \delta^4(p + q - k_1 - k_2) \\ &= + \int \frac{dk_2^+}{2\pi} 2\pi \delta(k_2^+) \\ &\quad \times \int \frac{dk_2^-}{2\pi} S_0(q - k_2) [-ig\gamma_\mu A_{\text{reg}}^{\mu a}(p + q - k_2)t^a] \\ &\quad \times \int \frac{d^2\mathbf{k}_{2\perp}}{(2\pi)^2} d^2\mathbf{x}_\perp e^{i\mathbf{k}_{2\perp}\mathbf{x}_\perp} \bar{u}(q)\gamma^+ [U_F(\mathbf{x}_\perp) - 1]v(p). \end{aligned} \quad (39)$$

In comparison with amplitude (b) (33), the above expression does not include a negative sign since the effective vertex $\mathcal{T}(k_2, q)$ (27) is inserted into the quark propagator, where $q^+ > 0$. However, both amplitudes are structured in the same way, so eq. (39) is solved following the same procedure as in the previous diagram. After performing the integration over k_1 with the four dimensional delta function, eq. (39) can be integrated over k_2^+ with the $\delta(k_2^+)$ -function and later over the momentum k_2^-

using the theorem of residues. It can be predictable that the only contribution from the regular field $A_{\text{reg}}^\mu(p+q-k_2)$ (18) is the proton field $A_p^\mu(p+q-k_2)$ (11), since diagram (c) is a reflection of diagram (b). This means that the two poles coming from the regular field $A_{\text{reg}}^\mu(p+q-k_2)$ (18) are located in the same upper plane of k_2^- , as well as the singularity of the quark propagator $S_0(q-k_2)$ (28), which is

$$\begin{aligned}
(q-k_2)^2 - m^2 + i\epsilon &= 0 \\
2(q^+ - k_2^+)(q^- - k_2^-) - (\mathbf{q}_\perp - \mathbf{k}_{2\perp})^2 - m^2 + i\epsilon &= 0 \\
2q^+(q^- - k_2^-) - (\mathbf{q}_\perp - \mathbf{k}_{2\perp})^2 - m^2 + i\epsilon &= 0 \\
\Rightarrow k_2^- &= q^- - \frac{(\mathbf{q}_\perp - \mathbf{k}_{2\perp})^2 + m^2}{2q^+} + \frac{i\epsilon}{2q^+}.
\end{aligned} \tag{40}$$

Therefore, the integration of the second term of the regular field $A_{\text{reg}}^\mu(p+q-k_2)$ (18) over k_2^- vanishes by the theorem of residues and the only non-zero contribution is the first term, that is, the proton field $A_p^\mu(p+q-k_2)$ (13) whose delta function in the form $\delta(p^- + q^- - k_2^-)$ can be used to solve the k_2^- -integral.

In order to conveniently sum the four diagrams at the end, the propagator $S_0(q-k_2)$ in eq. (39) is written as

$$\begin{aligned}
i \frac{\not{q} - \not{k}_2 + m}{(q-k_2)^2 - m^2 + i\epsilon} &= i \frac{\not{q} - \not{k}'_2 + m}{2(q^+ - k_2^+)(q^- - k_2^-) - (\mathbf{q}_\perp - \mathbf{k}_{2\perp})^2 - m^2 + i\epsilon} \\
&= i \frac{-\not{p} + \not{k}_1 + m}{2(q^+)(q^- - k_2^-) - (-\mathbf{p}_\perp + \mathbf{k}_{1\perp})^2 - m^2 + i\epsilon} \\
&= -i \frac{-\not{p} + \not{k}_1 + m}{2q^+p^- + (\mathbf{q}_\perp - \mathbf{k}_{2\perp})^2 + m^2 - i\epsilon}.
\end{aligned} \tag{41}$$

In contrast with the amplitude (b) in eq. (37), the minus sign of the propagator is kept in the final expression of the amplitude (c), which, after the change of variables $\mathbf{k}_{2\perp} = \mathbf{p}_\perp + \mathbf{q}_\perp - \mathbf{k}_{1\perp}$, reads

$$\begin{aligned}
\mathcal{M}_{(c)} &= -g^2 \int \frac{d^2\mathbf{k}_{1\perp}}{(2\pi)^2} \frac{\rho_p(\mathbf{k}_{1\perp})}{k_1^2} \int d^2\mathbf{x}_\perp e^{i(\mathbf{p}_\perp + \mathbf{q}_\perp - \mathbf{k}_{1\perp})\mathbf{x}_\perp} \\
&\quad \times \frac{\bar{u}(q)\gamma^+[U_F(\mathbf{x}_\perp) - 1](-\not{p} + \not{k}_1 + m)\gamma^- t^b v(p)}{2q^+p^- + (-\mathbf{p}_\perp + \mathbf{k}_{1\perp})^2 + m^2}.
\end{aligned} \tag{42}$$

Finally, diagram (d) contains two Wilson lines, $U_F(\mathbf{x}_\perp)$ and $U_F^\dagger(\mathbf{y}_\perp)$, in the quark and antiquark propagator, respectively. The contribution of this diagram can be

written as

$$\begin{aligned} \mathcal{M}_{(d)} = & \int \frac{d^4 k_2}{(2\pi)^4} \int \frac{d^4 k}{(2\pi)^4} \int \frac{d^4 k_1}{(2\pi)^4} (2\pi)^4 \delta^4(k_1 + k_2 - p - q) \bar{u}(q) \mathcal{T}(k, q) S_0(q - k) \\ & \times [-ig \mathcal{A}_{\text{reg}}(k_1) \cdot t] S_0(-p + (k_2 - k)) \mathcal{T}(k_2 - k, -p) v(p). \end{aligned} \quad (43)$$

Here, the momentum $k_2 - k$ transferred to the antiquark line is renamed as k_3 , to conveniently make an analogy between this amplitude and the (b) and (c) contributions later on.

Equation (43) can be solved first with the four dimensional delta function integrated over k_1 , where now the momentum conservation is $k_1 = -k - k_3 + p + q$. Then, the amplitude (d) in eq. (43) can be written as

$$\begin{aligned} \mathcal{M}_{(d)} = & - \int \frac{dk_3^+}{2\pi} (2\pi) \delta(k_3^+) \int \frac{dk^+}{2\pi} (2\pi) \delta(k^+) \\ & \times \int \frac{dk^-}{2\pi} \int \frac{dk_3^-}{2\pi} S_0(q - k) [-ig \mathcal{A}_{\text{reg}}(-k - k_3 + p + q) \cdot t] S_0(-p + k_3) \\ & \times \int \frac{d\mathbf{k}_\perp}{(2\pi)^2} \frac{d\mathbf{k}_{3\perp}}{(2\pi)^2} d^2 \mathbf{x}_\perp e^{i\mathbf{k}_\perp \cdot \mathbf{x}_\perp} d^2 \mathbf{y}_\perp e^{i\mathbf{k}_{3\perp} \cdot \mathbf{y}_\perp} \\ & \times \bar{u}(q) \gamma^+ [U_F(\mathbf{x}_\perp) - 1] \gamma^+ [U_F^\dagger(\mathbf{y}_\perp) - 1] v(p). \end{aligned} \quad (44)$$

Following the same procedure so far, eq. (44) can be solved starting with the integration over k^+ and k_3^+ . After that, the residue theorem can be applied to integrate over the minus component of the momentum considering the second term within the regular field $\mathcal{A}_{\text{reg}}^\mu(-k - k_3 + p + q)$ (18). The latter contains the following poles:

$$\begin{aligned} -k^- - k_3^- + p^- + q^- + i\epsilon &= 0 \\ \Rightarrow k_3^- &= -k^- + p^- + q^- + i\epsilon. \end{aligned} \quad (45)$$

$$\begin{aligned} & (-k - k_3 + p + q)^2 + (-k^+ - k_3^+ + p^+ + q^+) i\epsilon \\ \Rightarrow k_3^- &= -k^- + p^- + q^- - \frac{(-\mathbf{k}_\perp - \mathbf{k}_{3\perp} + \mathbf{p}_\perp + \mathbf{q}_\perp)^2}{2(-k^+ - k_3^+ + p^+ + q^+)} + \frac{i\epsilon}{2}. \end{aligned} \quad (46)$$

Here it can be seen that both singularities have the $+i\epsilon$ -prescription. The pole of the intermediate propagator $S_0(-p + k_3)$ in eq. (44) has already been found in eq. (34), exchanging k_2 momentum for k_3 . Thus, the k_3^- -integral vanishes by the residue theorem, since it is possible to close the contour of integration in the lower half plane of k_3^- , where there are no singularities.

The same result is valid in the integration over k^- because both cases are symmetric. To apply the residue theorem, the singularities within the regular field can be read by isolating the k momentum in eqs. (45) and (46). The pole of the intermediate propagator $S_0(q - k)$ in eq. (44) is the same as in eq. (40), exchanging the k_2 momentum for k .

As in the previous diagrams, only the proton field $A_p^\mu(k_1)$ (13) of the regular field $A_{\text{reg}}^\mu(k_1)$ (18) contributes to the integration over k_3^- and k^- in eq. (44). At this point, the change of variables is reverted and $p + q - k_1 - k$ is considered the momentum flowing from the nucleus to the antiquark line. Then, returning to expression (43), only one insertion of the proton field is considered,

$$\begin{aligned} \mathcal{M}_{(d)} = & - \int \frac{d^4 k}{(2\pi)^4} \int \frac{d^4 k_2}{(2\pi)^4} \int \frac{d^4 k_1}{(2\pi)^4} \delta(k_1 + k_2 - p - q) \delta(k^+) \delta(p^+ + q^+ - k^+ - k_1^+) \\ & \times \int d^2 \mathbf{x}_\perp e^{i\mathbf{k}_\perp \cdot \mathbf{x}_\perp} \int d^2 \mathbf{y}_\perp e^{i(p_\perp + q_\perp - \mathbf{k}_\perp - \mathbf{k}_{1\perp}) \cdot \mathbf{y}_\perp} \bar{u}(q) \gamma^+ [U_F(\mathbf{x}_\perp) - 1] S_0(q - k) \\ & \times [-ig A_p^\mu(k_1) \cdot t] S_0(-p + (p + q - k - k_1)) \gamma^+ [U_F^\dagger(\mathbf{y}_\perp) - 1] v(p). \end{aligned} \quad (47)$$

This expression can be solved by integrating first over k_2 with the delta-function in the form $\delta(k_1 + k_2 - p - q)$. Then, the integrals over k^+ and k_1^+ are solved with respectively the $\delta(k^+)$ and $\delta(p^+ + q^+ - k^+ - k_1^+)$ functions from the effective vertices $\mathcal{T}(k, p)$ and $\mathcal{T}(k_2 - k, -p)$, which are defined in eq. (27). The integration over k_1^- can be performed with the $\delta(k_1^-)$ function from the proton field. Finally, the k^- -integral is solved using the residue theorem.

The poles in the intermediate propagators $S_0(q - k)$ and $S_0(q - k - k_1)$ defined in eq. (28), respectively are

$$k^- = q^- - \frac{(\mathbf{q}_\perp - \mathbf{k}_\perp)^2 + m^2}{2q^+} + \frac{i\epsilon}{2q^+}, \quad (48)$$

$$k'^- = q^- + \frac{(\mathbf{q}_\perp - \mathbf{k}_\perp - \mathbf{k}_{1\perp})^2 + m^2}{2p^+} - \frac{i\epsilon}{2p^+}. \quad (49)$$

The integration over k^- can then be solved by choosing the contour of integration in

the lower half plane, which encloses the k'^- singularity in eq. (49),

$$\int \frac{dk^-}{2\pi} \frac{\not{q} - \not{k} + m}{(q-k)^2 - m^2} \frac{\not{q} - \not{k} - \not{k}_1 + m}{(q-k-k_1)^2 - m^2} = -2\pi i [\text{Res}(k^- = q^- + ((\mathbf{q}_\perp - \mathbf{k}_\perp - \mathbf{k}_{1\perp})^2 + m^2 - i\epsilon)/2p^+)] . \quad (50)$$

Excluding the numerators of the integrand in eq. (50), the residue is

$$\begin{aligned} & \text{Res}(k^- = q^- + ((\mathbf{q}_\perp - \mathbf{k}_\perp - \mathbf{k}_{1\perp})^2 + m^2 - i\epsilon)/2p^+) \\ &= \lim_{k^- \rightarrow k'^-} \frac{k^- - \left\{ q^- + \frac{(\mathbf{q}_\perp - \mathbf{k}_\perp - \mathbf{k}_{1\perp})^2 + m^2 - i\epsilon}{2p^+} \right\}}{[(q-k)^2 - m^2] \left[2p^+ \left(k^- - \left\{ q^- + \frac{(\mathbf{q}_\perp - \mathbf{k}_\perp - \mathbf{k}_{1\perp})^2 + m^2 - i\epsilon}{2p^+} \right\} \right) \right]} \\ &= \lim_{k^- \rightarrow k'^-} \frac{1}{[2(q^+)(q^- - k^-) - (\mathbf{q}_\perp - \mathbf{k}_\perp)^2 - m^2] 2p^+} \\ &= \frac{1}{[2(q^+)(q^- - q^- - \frac{(\mathbf{q}_\perp - \mathbf{k}_\perp - \mathbf{k}_{1\perp})^2 + m^2}{2p^+}) - (\mathbf{q}_\perp - \mathbf{k}_\perp)^2 - m^2] 2p^+} \\ &= \frac{1}{-2q^+(\mathbf{q}_\perp - \mathbf{k}_\perp - \mathbf{k}_{1\perp})^2 + m^2 - 2p^+((\mathbf{q}_\perp - \mathbf{k}_\perp)^2 + m^2)} \\ &= \frac{1}{-2q^+[(\mathbf{q}_\perp - \mathbf{k}_\perp - \mathbf{k}_{1\perp})^2 + m^2] - 2p^+[(\mathbf{q}_\perp - \mathbf{k}_\perp)^2 + m^2]} . \end{aligned} \quad (51)$$

With the result in eq. (51), the solution of the k^- -integral is

$$\int \frac{dk^-}{2\pi} \frac{\not{q} - \not{k} + m}{(q-k)^2 - m^2} \frac{\not{q} - \not{k} - \not{k}_1 + m}{(q-k-k_1)^2 - m^2} = -i \frac{(\not{q} - \not{k} + m)(\not{q} - \not{k} - \not{k}_1 + m)}{2q^+[(\mathbf{q}_\perp - \mathbf{k}_\perp - \mathbf{k}_{1\perp})^2 + m^2] + 2p^+[(\mathbf{q}_\perp - \mathbf{k}_\perp)^2 + m^2]} . \quad (52)$$

Including this result in the final expression of amplitude (d), this reads,

$$\begin{aligned} \mathcal{M}_{(d)} &= g^2 \int \frac{d^2 \mathbf{k}_{1\perp}}{(2\pi)^2} \frac{d^2 \mathbf{k}_\perp}{(2\pi)^2} \frac{\rho_{p,a}(\mathbf{k}_{1\perp})}{k_{1\perp}^2} \int d^2 \mathbf{x}_\perp d^2 \mathbf{y}_\perp e^{i\mathbf{k}_\perp \mathbf{x}_\perp} e^{i(\mathbf{p}_\perp + \mathbf{q}_\perp - \mathbf{k}_\perp - \mathbf{k}_{1\perp}) \mathbf{y}_\perp} \\ &\times \frac{\bar{u}(q) \gamma^+ [U_F(\mathbf{x}_\perp) - 1] (\not{q} - \not{k} + m) \gamma^- t^a (\not{q} - \not{k} - \not{k}_1 + m) \gamma^+ [U_F^\dagger(\mathbf{y}_\perp) - 1] v(p)}{2q^+[(\mathbf{q}_\perp - \mathbf{k}_\perp - \mathbf{k}_{1\perp})^2 + m^2] + 2p^+[(\mathbf{q}_\perp - \mathbf{k}_\perp)^2 + m^2]} . \end{aligned} \quad (53)$$

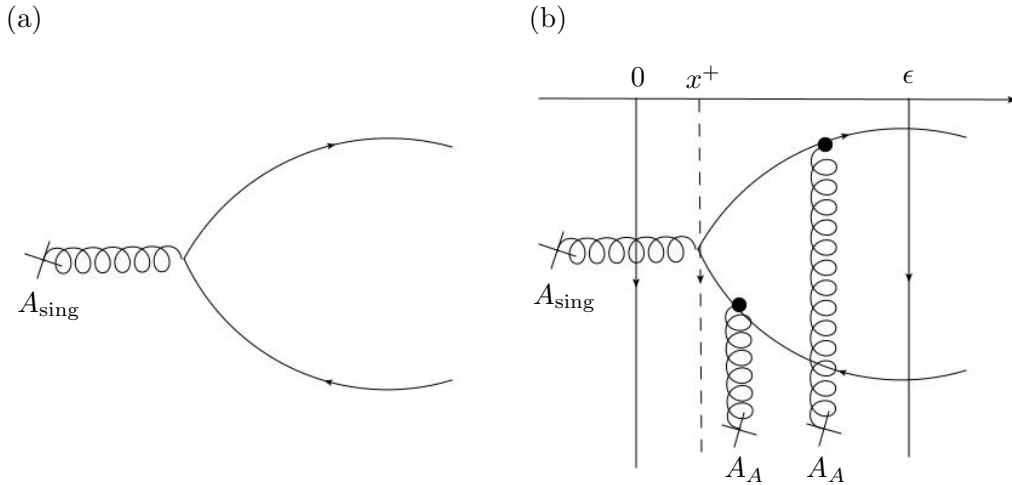


Figure 5. Diagram (a) represents the pair production from the singular term. Diagram (b) shows the regularized region, where the interaction in the x^+ coordinate is extended from 0 to ϵ . The gluon line ended with a cross denotes a classical field insertion. The black dot represents the effective vertex in eq. (27).

3.2.2 Singular term

The production of a $q\bar{q}$ -pair from the singular term in eq. (17) is represented by diagram (a) in Figure 5. The production amplitude is calculated in coordinate space, where the singular field (25) is proportional to $\delta(x^+)$, and thus, the physical interpretation of this amplitude is the production of the quark pair inside the nucleus. Without regularization, the contribution of the singular amplitude would be the same as the regular amplitude (a) in eq. (29), exchanging the regular field $A_{\text{reg}}^\mu(k_1)$ (18) for the singular field $A_{\text{sing}}^\mu(k_1)$ (25). However, the $\delta(x^+)$ function is regularized by giving a small width to the nucleus,

$$\delta(x^+) \rightarrow \delta_\epsilon(x^+) . \quad (54)$$

Here $\delta_\epsilon(x^+)$ is a regular function whose support is $[0, \epsilon]$ and it becomes a $\delta(x^+)$ when ϵ goes to zero. This allows the $q\bar{q}$ -pair to undergo multiple gluon scatterings between the “time” x^+ , when the field A_{sing}^μ is inserted into the quark line, and ϵ (diagram (b) in Figure 5).

Therefore, the scattering of the quark-antiquark pair has to be treated differently than the regular contribution since it occurs inside the regularized region. In this case, it is necessary to use the incomplete Wilson lines of eq. (26). Then, the singular

amplitude in coordinate space is

$$\begin{aligned} \mathcal{M}_{\text{sing}} = & \int d^4x e^{i(p+q)x} \bar{u}(q) U_F(+\infty, x^+; \mathbf{x}_\perp) \\ & \times [ig A_{\text{sing}}(x) \cdot t] U_F^\dagger(+\infty, x^+; \mathbf{x}_\perp) v(p) . \end{aligned} \quad (55)$$

As in the previous regular amplitude, the above expression results from summing four possible singular contributions by replacing $U_F - 1$ by U_F and $U_F^\dagger - 1$ by U_F^\dagger . It can be seen in eq. (55) that the singular field insertion and the rescattering occur in the same transverse plane \mathbf{x}_\perp inside a heavily boosted nucleus. This is because of the vanishing duration of the interaction in the $\epsilon \rightarrow 0$ limit [16].

With the following identity,

$$U_F(+\infty, x^+; \mathbf{x}_\perp) t^a U_F^\dagger(+\infty, x^+; \mathbf{x}_\perp) = t^b U_A^{ba}(+\infty, x^+; \mathbf{x}_\perp) , \quad (56)$$

and the explicit form of the singular field $A_{\text{sing}}^-(x)$ (25), the singular amplitude (55) can be written as

$$\begin{aligned} \mathcal{M}_{\text{sing}} = & ig^2 \int dx^- d^2\mathbf{x}_\perp e^{i(p^++q^+)x^-} e^{-i(\mathbf{p}_\perp+\mathbf{q}_\perp)\mathbf{x}_\perp} \\ & \times \left\{ i \frac{g}{2} \int_{-\infty}^{\infty} dx^+ [U_A(+\infty, x^+; \mathbf{x}_\perp) A_A^-(x) \cdot TV(x^+, -\infty; \mathbf{x}_\perp)]_{ab} \right\} \\ & \times \bar{u}(q) \gamma^+ t^a \theta(x^-) \frac{1}{\nabla_\perp^2} \rho_{p,b}(\mathbf{x}_\perp) v(p) . \end{aligned} \quad (57)$$

Here the approximation $e^{i(p^-+q^-)x^-} \approx 1$ has been made because of the extension of the regularized region ($0 < x^+ < \epsilon$) in the x^+ -integral. The Heaviside function in eq. (57) can be Fourier transformed with the x^- -integral,

$$\tilde{\theta}(p^+ + q^+) = -\frac{1}{i(p^+ + q^+)} + \sqrt{2\pi} \sqrt{\frac{\pi}{2}} \delta(p^+ + q^+) . \quad (58)$$

Furthermore, the following formula [16] can be used to simplify eq. (57),

$$i \frac{g}{2} \int_{-\infty}^{\infty} dx^+ [U_A(+\infty, x^+; \mathbf{x}_\perp) A_A^-(x) \cdot TV(x^+, -\infty; \mathbf{x}_\perp)] = U_A(\mathbf{x}_\perp) - V(\mathbf{x}) . \quad (59)$$

Lastly, the color density of the proton $\rho_p(\mathbf{x}_\perp)$ can be Fourier transformed and with the Green's function of the Laplacian in momentum space, the singular amplitude

can be written as

$$\begin{aligned} \mathcal{M}_{\text{sing}} = g^2 \int \frac{d^2 \mathbf{k}_{1\perp}}{(2\pi)^2} \frac{\rho_{p,a}(\mathbf{k}_{1\perp})}{k_{1\perp}^2} d^2 \mathbf{x}_{\perp} e^{i(\mathbf{p}_{\perp} + \mathbf{q}_{\perp} - \mathbf{k}_{1\perp}) \mathbf{x}_{\perp}} \\ \times \frac{\bar{u}(q) \gamma^+ t^b v(p)}{p^+ + q^+} \left([V(\mathbf{x}_{\perp}) - 1]_{ba} - [U_A(\mathbf{x}_{\perp}) - 1]_{ba} \right). \end{aligned} \quad (60)$$

3.2.3 Complete time-ordered amplitude

The complete amplitude of $q\bar{q}$ -production is obtained by summing the regular and singular contributions in eqs. (31), (37), (42), (53) and (60). In this sum, the Wilson Line $V(\mathbf{x}_{\perp})$ is cancelled by the contributions (31) and (60). The (b) and (c) amplitudes in eqs. (37) and (42) respectively cancel with the $[U_F^{\dagger}(\mathbf{x}_{\perp}) - 1]$ and $[U_F(\mathbf{x}_{\perp}) - 1]$ terms of the amplitude (d) (53) after using the identities [16]

$$\begin{aligned} \bar{u}(q) \gamma^- &= \frac{1}{2q^+} \bar{u}(q) \gamma^+ (\not{q} + m) \gamma^-, \\ \gamma^- v(p) &= \frac{1}{2p^+} \gamma^- (\not{p} - m) \gamma^+ v(p). \end{aligned} \quad (61)$$

Lastly, there is also a cancellation among the first term without the Wilson Line $U_A(\mathbf{x}_{\perp})$ in amplitude (a) (31), the singular amplitude (60) and the term without the Wilson Lines $U_F(\mathbf{x}_{\perp})$ and $U_F^{\dagger}(\mathbf{y}_{\perp})$ in amplitude (d) (53).

The terms that survive the above mentioned cancellations give the complete quark pair production amplitude in covariant gauge, which is written as

$$\begin{aligned} \mathcal{M}_{g \rightarrow q\bar{q}}^{\text{cov}} = g \int \frac{d^2 \mathbf{k}_{1\perp}}{(2\pi)^2} \frac{d^2 \mathbf{k}_{\perp}}{(2\pi)^2} \frac{g \rho_{p,a}(\mathbf{k}_{1\perp})}{k_{1\perp}^2} \int d^2 \mathbf{x}_{\perp} d^2 \mathbf{y}_{\perp} e^{i\mathbf{k}_{\perp} \mathbf{x}_{\perp}} e^{i(\mathbf{p}_{\perp} + \mathbf{q}_{\perp} - \mathbf{k}_{\perp} - \mathbf{k}_{1\perp}) \mathbf{y}_{\perp}} \\ \times \left\{ \frac{\bar{u}(q) \gamma^+ (\not{q} - \not{k} + m) \gamma^- (\not{q} - \not{k} - \not{k}_1 + m) \gamma^+ [U_F(\mathbf{x}_{\perp}) t^a U_F^{\dagger}(\mathbf{y}_{\perp})] v(p)}{2p^+ [(\mathbf{q}_{\perp} - \mathbf{k}_{\perp})^2 + m^2] + 2q^+ [(\mathbf{q}_{\perp} - \mathbf{k}_{\perp} - \mathbf{k}_{1\perp})^2 + m^2]} \right. \\ \left. + \bar{u}(q) \left[\frac{\not{q} U(p + q, \mathbf{k}_{1\perp})}{(p + q)^2} - \frac{\gamma^+}{p^+ + q^+} \right] t^b U_A^{ba}(\mathbf{x}_{\perp}) v(p) \right\}. \end{aligned} \quad (62)$$

In this expression, it is possible to interpret the first term as the splitting of a gluon into a $q\bar{q}$ -pair and the subsequent interaction of the $q\bar{q}$ -state with the nucleus, which is expressed with the two Wilson Lines in the fundamental representation at two different transverse coordinates, $U_F(\mathbf{x}_{\perp})$ and $U_F^{\dagger}(\mathbf{y}_{\perp})$.

The second term in eq. (62) can be rewritten as [16],

$$\bar{u}(q) \left[\frac{\mathcal{C}'_U(p+q, \mathbf{k}_{1\perp})}{(p+q)^2} - \frac{\gamma^+}{p^+ + q^+} \right] t^b v(p) = \bar{u}(q) \frac{\mathcal{C}'_L(p+q, \mathbf{k}_{1\perp})}{(p+q)^2} t^b v(p), \quad (63)$$

where $\mathcal{C}'_L(p+q, \mathbf{k}_{1\perp})$ is the effective Lipatov vertex [19, 20] which resums all the diagrams that contribute to the production of a gluon with momentum $p+q$ via the fusion of two gluons with momenta k_1 and $p+q-k_1$ in the high energy limit. Its components are

$$C_L^+(p+q, \mathbf{k}_{1\perp}) = (p^+ + q^+) - \frac{\mathbf{k}_{1\perp}^2}{p^- + q^- + i\epsilon}, \quad (64)$$

$$C_L^-(p+q, \mathbf{k}_{1\perp}) = \frac{(\mathbf{p}_\perp + \mathbf{q}_\perp - \mathbf{k}_{1\perp})^2}{p^+ + q^+} - (p^- + q^-), \quad (65)$$

$$C_{L\perp}(p+q, \mathbf{k}_{1\perp}) = \mathbf{p}_\perp + \mathbf{q}_\perp - 2\mathbf{k}_{1\perp}. \quad (66)$$

Thus, the second term in eq. (62) can be physically interpreted as a valence quark in the proton emitting a gluon that interacts first with the gluon condensate in the nucleus and emits the quark pair afterwards, outside the nucleus. The interaction is represented by the adjoint Wilson Line $U_A(\mathbf{x}_\perp)$.

Finally, the covariant amplitude can be written as

$$\begin{aligned} \mathcal{M}_{g \rightarrow q\bar{q}}^{\text{cov}} = & g \int \frac{d^2 \mathbf{k}_{1\perp}}{(2\pi)^2} \frac{d^2 \mathbf{k}_\perp}{(2\pi)^2} \frac{g\rho_{p,a}(\mathbf{k}_{1\perp})}{k_{1\perp}^2} \int d^2 \mathbf{x}_\perp d^2 \mathbf{y}_\perp e^{i\mathbf{k}_\perp \mathbf{x}_\perp} e^{i(\mathbf{p}_\perp + \mathbf{q}_\perp - \mathbf{k}_\perp - \mathbf{k}_{1\perp}) \mathbf{y}_\perp} \\ & \times \bar{u}(q) \left\{ T_{q\bar{q}}(\mathbf{k}_{1\perp}, \mathbf{k}_\perp) [U_F(\mathbf{x}_\perp) t^a U_F^\dagger(\mathbf{y}_\perp)] + T_g(\mathbf{k}_{1\perp}) [t^b U_A^{ba}(\mathbf{x}_\perp)] \right\} v(p), \end{aligned} \quad (67)$$

where

$$T_{q\bar{q}}(\mathbf{k}_{1\perp}, \mathbf{k}_\perp) \equiv \frac{\gamma^+(\not{q} - \not{k} + m) \gamma^-(\not{q} - \not{k} - \not{k}_1 + m) \gamma^+}{2p^+ [(\mathbf{q}_\perp - \mathbf{k}_\perp)^2 + m^2] + 2q^+ [(\mathbf{q}_\perp - \mathbf{k}_\perp - \mathbf{k}_{1\perp})^2 + m^2]}, \quad (68)$$

$$T_g(\mathbf{k}_{1\perp}) \equiv \frac{\mathcal{C}'_L(p+q, \mathbf{k}_{1\perp})}{(p+q)^2}. \quad (69)$$

4 Pair production in Light Cone Perturbation Theory

In light cone perturbation theory the incoming gluon emitted from a valence quark in the dilute proton and the outgoing quark pair are defined as a perturbative series of Fock states. These bare states eikonally interact with the classical color field of the nucleus and this interaction is represented by Wilson lines in mixed space, where the kinematics of a particle is described by its light cone longitudinal momentum k^+ and transverse position \mathbf{x}_\perp .

In this second part of the thesis, the pair production amplitude $\mathcal{M}_{g \rightarrow q\bar{q}}$ is calculated from the matrix elements of the initial and final dressed states using light cone quantization [21]

$${}_D \langle q(k_2) \bar{q}(k_3) | \hat{\mathcal{S}}_E - \mathbf{1} | g(k_1) \rangle_D = 2k_1^+ (2\pi) \delta(k_1^+ - k_2^+ - k_3^+) i \mathcal{M}_{g \rightarrow q\bar{q}}, \quad (70)$$

where $\hat{\mathcal{S}}_E$ is the eikonal scattering operator describing a color rotation of a parton (quarks and gluons) in the target color field. In contrast with the previous calculation, the polarization of the incoming gluon is considered explicitly.

4.1 Perturbative Fock state expansion

In interacting field theory, the light cone Hamiltonian \hat{P}^- can be split into the kinetic and interacting terms $\hat{P}^- = \hat{T} + \hat{V}_I$ [22]. In the interaction picture, the free Hamiltonian \hat{T} generates the x^+ -evolution of operators,

$$\hat{\mathcal{O}}_I(x^+) = e^{i\hat{T}x^+} \hat{\mathcal{O}}_I(0) e^{-i\hat{T}x^+}, \quad (71)$$

and the states evolve with the interacting Hamiltonian \hat{V}_I :

$$|i(x_2^+)\rangle_I = \mathcal{P} \exp\left(-i \int_{x_1^+}^{x_2^+} dx^+ \hat{V}_I(x^+)\right) |i(x_1^+)\rangle, \quad (72)$$

where \mathcal{P} indicates the ordering of the operators $\hat{V}_I(x^+)$ along the x^+ -coordinate. By convention, states in the interaction picture are defined in such a way that they coincide at $x^+ = 0$ with the corresponding states in the Heisenberg picture, i.e. $|i(0)\rangle_I \equiv |i\rangle_H$. Thus, the evolution of the interaction state from $x_1^+ = -\infty$ to $x_2^+ = 0$ can be written as [23]

$$|i\rangle_H = \mathcal{P} \exp\left(-i \int_{-\infty}^0 dx^+ \hat{V}_I(x^+)\right) |i(-\infty)\rangle_I. \quad (73)$$

In perturbation theory, the state $|i(-\infty)\rangle_I$ can be considered as a free state since it comes before any insertion of the interaction operator $\hat{V}_I(x^+)$. This free state is called bare or asymptotic state whereas the physical state $|i\rangle_H$ is known as dressed state.

When the dressed state is one-particle state, it can be expanded over a basis of Fock states $|\mathcal{F}\rangle$ [6],

$$|i\rangle_H = \sqrt{Z_i} \left[|i(-\infty)\rangle_I + \sum_{\mathcal{F} \neq i} |\mathcal{F}\rangle \Psi_{i \rightarrow \mathcal{F}} \right], \quad (74)$$

where the sum contains the quantum numbers of each parton in the Fock state and a phase space integration,

$$\int_0^\infty \frac{dk^+}{2k^+(2\pi)} \int \frac{d^2 \mathbf{k}_\perp}{(2\pi)^2}. \quad (75)$$

However, the sum in eq. (74) excludes the state $|i(-\infty)\rangle_I$ proportional to the physical state $|i\rangle_H$. The $\sqrt{Z_i}$ factor in eq. (74) is the wave-function renormalization constant and the coefficients of the expansion are light cone wave functions (LCWFs) $\Psi_{i \rightarrow \mathcal{F}}$ defined as

$$\Psi_{i \rightarrow \mathcal{F}} = \langle \mathcal{F} | i \rangle_H = \langle \mathcal{F} | \mathcal{P} \exp\left(-i \int_{-\infty}^0 dx^+ \hat{V}_I(x^+)\right) | i(-\infty) \rangle_I. \quad (76)$$

The above expression can be rewritten using eq. (71) to extract the x^+ dependence from $\hat{V}_I(x^+)$ and then expanding the exponentials [23]. Further, inserting various times the decomposition of the identity

$$\mathbf{1} = \sum_{\mathcal{F}} |\mathcal{F}\rangle \langle \mathcal{F}|, \quad (77)$$

the LCWFs can be written in the form of the following perturbative expansion [23],

$$\begin{aligned} \Psi_{i \rightarrow \mathcal{F}} &= \frac{\langle \mathcal{F} | \hat{V}_I(0) | i(-\infty) \rangle_I}{T_i - T_{\mathcal{F}} + i\epsilon} \\ &+ \sum_{n=2}^{\infty} \sum_{\mathcal{F}_{n-1} \neq i} \cdots \sum_{\mathcal{F}_1 \neq i} \frac{1}{T_i - T_{\mathcal{F}} + i\epsilon} \langle \mathcal{F} | \hat{V}_I(0) | \mathcal{F}_{n-1} \rangle \frac{1}{T_i - T_{\mathcal{F}_{n-1}} + i\epsilon} \cdots \\ &\cdots \frac{1}{T_i - T_{\mathcal{F}_1} + i\epsilon} \langle \mathcal{F} | \hat{V}_I(0) | i(-\infty) \rangle_I, \end{aligned} \quad (78)$$

where $T_i = k_i^- \equiv (\mathbf{k}_{i\perp}^2 + m_i^2)/(2k_i^+)$ is the eigenvalue of \hat{T} corresponding to the state $|i(-\infty)\rangle_I$.

Hence, the Fock state expansion for the physical states in the interaction picture has the form of the quantum mechanical expansion in perturbation theory [21],

$$|\Psi\rangle_I = \sqrt{Z_{\Psi}} \left[|\Psi\rangle + \sum_{n_1}' \frac{\langle n_1 | H' | \Psi \rangle}{E_{\Psi} - E_1} |n_1\rangle + \sum_{n_1, n_2}' \frac{\langle n_2 | H' | n_1 \rangle \langle n_1 | H' | \Psi \rangle}{(E_{\Psi} - E_2)(E_{\Psi} - E_1)} |n_2\rangle + \dots \right], \quad (79)$$

where the prime in the sum symbol \sum' indicates that the intermediate state proportional to $|\Psi\rangle$ is excluded of the sum.

The wave function renormalization Z_{Ψ} contains ultraviolet divergences appearing in loop diagrams and it can be calculated either by calculating the incoming particle propagator correction diagrams or from the normalization requirement [24]

$${}_I\langle \Psi | \Psi \rangle_I = \langle \Psi(q, s) | \Psi(p, s) \rangle = 2p^+ (2\pi)^3 \delta(p^+ - q^+) \delta^2(\mathbf{p} - \mathbf{q}) \delta_{ss'}, \quad (80)$$

so that,

$$Z_{\Psi}^{-1} = 1 + \frac{1}{\langle \Psi | \Psi \rangle} \sum_n' \frac{|\langle n | H | \Psi \rangle|^2}{(E_{\Psi} - E_n)^2} + \dots \quad (81)$$

However, the pair production amplitude at LO in the strong coupling constant does not include any loop contributions so that the renormalization constant is one.

4.2 Initial and final Fock states in mixed space

In the high energy scattering of a dense target, the most convenient representation is the mixed state coordinates (k^+, \mathbf{x}_\perp) where states and operators are obtained from the full momentum-space representation (k^+, \mathbf{k}_\perp) by a transverse Fourier transform. For example, the mixed-space Fock state $|\widetilde{\mathcal{F}}\rangle$ is obtained from its analog in momentum space $|\mathcal{F}\rangle$ as [23]

$$|\widetilde{\mathcal{F}}\rangle = \int \left[\prod_{l \in \mathcal{F}} \frac{d\mathbf{k}_{l\perp}}{(2\pi)^2} e^{-i\mathbf{k}_{l\perp} \mathbf{x}_{l\perp}} \right] |\mathcal{F}\rangle, \quad (82)$$

where the product is over each parton l present in $|\mathcal{F}\rangle$.

To calculate the $q\bar{q}$ production amplitude in eq. (70), it is necessary to decompose the dressed gluon state $|g\rangle_D$ corresponding to one physical particle state in the interaction picture in terms of the free/bare states $|\dots\rangle_0$, as it is presented in eq. (74). In mixed space, this expansion is given by

$$|\widetilde{g_1}\rangle_D = \sqrt{Z_g} \left[|\widetilde{g_1}\rangle_0 + \sum_{q_2 \bar{q}_3} \widetilde{\Psi}_{g \rightarrow q_2 \bar{q}_3} |\widetilde{q_2 \bar{q}_3}\rangle_0 + \dots \right], \quad (83)$$

where $g_1 = g(k_1^+, \mathbf{x}_{1\perp}, \lambda, a)$, $q_2 = q(k_2^+, \mathbf{x}_{2\perp}, h_2, \alpha_2)$ and $\bar{q}_3 = \bar{q}(k_3^+, \mathbf{x}_{3\perp}, h_3, \alpha_3)$. Here, λ and a are respectively the polarization and color of the gluon and h_i and α_i are the helicities and colors of the quark ($i = 2$) and antiquark ($i = 3$).

In the expansion (83), the renormalization coefficient $Z_g = 1 + \mathcal{O}(g^2)$ will be omitted as well as the next-to-leading order (NLO) Fock states denoted by (\dots) . The symbol $\widetilde{\sum}$ is the two particle phase space sum over the $q\bar{q}$ -Fock states in mixed space. It is given by [25]

$$\widetilde{\sum}_{q_2 \bar{q}_3} = \sum_{h_2, \alpha_2, f_2} \sum_{h_3, \alpha_3, f_3} \prod_{i=2}^3 \left[\int_{-\infty}^{\infty} \frac{dk_i^+}{2\pi} \frac{\theta(k_i^+)}{2k_i^+} (2\pi) \delta\left(k_1^+ - \sum_{j=2}^3 k_j^+\right) \int d^2 \mathbf{x}_{i\perp} \right]. \quad (84)$$

In the following calculations, the helicity h , color α and quark flavour f indices are left implicit, summed over when appropriate. The light cone wavefunction $\widetilde{\Psi}_{g \rightarrow q\bar{q}}$ is calculated in the next subsection 4.3 using Light Cone Perturbation theory.

The bare states in eq. (83) are conveniently written using the creation operators $\tilde{a}_1^\dagger = a^\dagger(k_1^+, \mathbf{x}_{1\perp}, \lambda_1, a)$ for the gluon, $\tilde{b}_2^\dagger = b^\dagger(k_2^+, \mathbf{x}_{2\perp}, h_2, \alpha_2)$ for the quark, and $\tilde{d}_3^\dagger =$

$d^\dagger(k_3^+, \mathbf{x}_{3\perp}, h_3, \alpha_3)$ for the antiquark:

$$\widetilde{|g_1\rangle}_D = \sqrt{Z_g} \left[\widetilde{a_1^\dagger|0\rangle}_0 + \sum_{q_2 \bar{q}_3 \text{ F. s.}} \widetilde{\Psi}_{g \rightarrow q_2 \bar{q}_3} \widetilde{b_2^\dagger \bar{d}_3^\dagger|0\rangle}_0 + \dots \right]. \quad (85)$$

These operators \tilde{a} , \tilde{b} and \tilde{d} satisfy the following (anti-)commutation relations,

$$\begin{aligned} \left[\tilde{a}(k^+, \mathbf{x}_\perp, \lambda, a), \tilde{a}^\dagger(q^+, \mathbf{y}_\perp, \sigma, b) \right] &= (2k^+)(2\pi) \delta(k^+ - q^+) \delta^{(2)}(\mathbf{x}_\perp - \mathbf{y}_\perp) \delta_{\lambda\sigma} \delta_{ab}, \\ \left\{ \tilde{b}(k^+, \mathbf{x}_\perp, h, \alpha), \tilde{b}^\dagger(q^+, \mathbf{y}_\perp, s, \beta) \right\} &= (2k^+)(2\pi) \delta(k^+ - q^+) \delta^{(2)}(\mathbf{x}_\perp - \mathbf{y}_\perp) \delta_{hs} \delta_{\alpha\beta}, \\ \left\{ \tilde{d}(k^+, \mathbf{x}_\perp, h, \alpha), \tilde{d}^\dagger(q^+, \mathbf{y}_\perp, s, \beta) \right\} &= (2k^+)(2\pi) \delta(k^+ - q^+) \delta^{(2)}(\mathbf{x}_\perp - \mathbf{y}_\perp) \delta_{hs} \delta_{\alpha\beta}. \end{aligned} \quad (86)$$

Finally, the outgoing quark pair state is expanded in terms of the Fock state basis as

$$\begin{aligned} {}_D \langle \widetilde{q_2' \bar{q}_3'} | &= \sqrt{Z_q} \sqrt{Z_{\bar{q}}} \left[{}_0 \langle \widetilde{q_2' \bar{q}_3'} | + \sum_{g_1'} {}_0 \langle \widetilde{g_1'} | \widetilde{\Psi}_{q_2' \bar{q}_3' \rightarrow g_1'}^\dagger + \dots \right] \\ &= \sqrt{Z_q} \sqrt{Z_{\bar{q}}} \left[{}_0 \langle 0 | \tilde{d}_{3'}^\dagger \tilde{b}_{2'} + \sum_{g_1'} {}_0 \langle 0 | \tilde{a}_{1'} \tilde{\Psi}_{q_2' \bar{q}_3' \rightarrow g_1'}^\dagger + \dots \right], \end{aligned} \quad (87)$$

where $\tilde{a}_{1'}^\dagger = a^\dagger(k_1^{+'}, \mathbf{x}'_{1\perp}, \lambda_1', a')$, $\tilde{b}_{2'}^\dagger = b^\dagger(k_2^{+'}, \mathbf{x}'_{2\perp}, h_2', \alpha_2')$ and $\tilde{d}_{3'}^\dagger = d^\dagger(k_3^{+'}, \mathbf{x}'_{3\perp}, h_3', \alpha_3')$. The symbol $\sum_{g_1'}$ is the one particle phase space of the gluon.

The relation between the gluon splitting wave function and the quark-antiquark merging wave function can be derived by the orthogonality of the Fock states in eqs. (83) and (87),

$$\begin{aligned} {}_D \langle \widetilde{q_2' \bar{q}_3'} | g_1 \rangle_D &= 0 \\ \left({}_0 \langle \widetilde{q_2' \bar{q}_3'} | + {}_0 \langle \widetilde{g_1'} | \widetilde{\Psi}_{q_2' \bar{q}_3' \rightarrow g_1'}^\dagger \right) \left(\widetilde{|g_1\rangle}_0 + \sum_{q_2 \bar{q}_3} \widetilde{\Psi}_{g \rightarrow q_2 \bar{q}_3} \widetilde{|q_2 \bar{q}_3\rangle}_0 \right) &= 0 \\ \Rightarrow \widetilde{\Psi}_{q_2' \bar{q}_3' \rightarrow g_1'}^\dagger &= -\widetilde{\Psi}_{g_1' \rightarrow q_2' \bar{q}_3'}. \end{aligned} \quad (88)$$

The result above indicates that both waves functions corresponding to the splitting and merging of partons are related by a minus sign in the time reversal transformation at LO.

4.3 Light cone wave function

The light cone wavefunction $\tilde{\Psi}_{g_1 \rightarrow q_2 \bar{q}_3}$ (78) can be calculated by determining the interaction vertex $\langle q\bar{q}|\hat{V}_I(0)|g\rangle$. One way to solve it is by calculating the interaction operator $\hat{V}_I(x^+)$ in QCD [22], inserting in $\hat{V}_I(0)$ the expressions of the free quantized fields in terms of creation and annihilation operators (see Appendix A of ref. [23]) and using commutation relations (86).

However, similarly as the procedure of applying Feynman rules for solving scattering diagrams, the LCWF can be obtained with the following LCPT rules [14, 26]:

1. Draw the x^+ ordered diagram at the desired order in the coupling g and assign a four-momentum k^μ to each line such that it is on mass shell ($k^2 = m^2$).
2. Similarly to the Feynman rules, the quark-gluon vertex is (i and j are quark color indices):

$$= -g \bar{u}_{\sigma' j}(k+q) \not{\epsilon}_\lambda(q) (t^a)_{ji} u_{\sigma i}(k), \quad (89)$$

where the light cone time flows from left to right. This vertex also includes the factors $(2\pi)^2 \delta^{(2)}(\mathbf{k}_{\perp \text{initial}} - \mathbf{k}_{\perp \text{final}})$ and $(2\pi) \delta(k_{\text{initial}}^+ - k_{\text{final}}^+)$ since only the k^+ and \mathbf{k}_\perp components of the four-momentum are conserved in each vertex.

3. For each intermediate state include a LC energy denominator factor

$$\frac{1}{\sum_{inc} k^- - \sum_{interm} k^-}, \quad (90)$$

where the sum \sum_{inc} runs over all incoming particles present in the initial state and the sum \sum_{interm} over all the particles in the corresponding intermediate state. Since the k^- momentum component is not conserved at the vertices, the light cone denominator is non-zero.

4. For each independent momentum k^μ integrate with the measure

$$\int \frac{dk^+ \theta(k^+)}{2k^+ (2\pi)} \frac{d^2 \mathbf{k}_\perp}{(2\pi)^2} . \quad (91)$$

5. Sum over all internal quark and gluon polarizations and colors.

The light cone wave function describes the vertex where the gluon splits into two quarks, but it is not the complete scattering process. Thus, the external final state of the quark pair is treated as an intermediate state since it undergoes subsequent interactions with the CGC of the nucleus after the splitting [14].

Following the LCPT rules, the LCWF for the gluon splitting $g(k_1) \rightarrow q(k_2)\bar{q}(k_3)$ in momentum space is

$$\begin{aligned} \Psi_{g \rightarrow q\bar{q}} &= \frac{{}_0\langle q_2 \bar{q}_3 | \hat{V}_I(0) | g_1 \rangle_0}{\Delta E} \\ &= \frac{-g}{k_1^- - (k_2^- + k_3^-)} \bar{u}_{h_2 \alpha_2}(k_2) \not{\epsilon}_\lambda(t^a)_{\alpha_2 \alpha_3} v_{h_3 \alpha_3}(k_3) . \end{aligned} \quad (92)$$

The Fourier transformed wave function $\tilde{\Psi}_{g \rightarrow q\bar{q}}$ in mixed space is

$$\tilde{\Psi}_{g \rightarrow q\bar{q}} = \int \frac{d^2 \mathbf{k}_{2\perp}}{(2\pi)^2} \int \frac{d^2 \mathbf{k}_{3\perp}}{(2\pi)^2} e^{-ik_2 x_2 - ik_3 x_3} (2\pi)^2 \delta^2(\mathbf{k}_{1\perp} - \mathbf{k}_{2\perp} - \mathbf{k}_{3\perp}) \Psi_{g \rightarrow q\bar{q}} . \quad (93)$$

Note that the (+)-momentum integrals in rule 5, the delta functions imposing (+)-momentum conservation in rule 2 and the sum over internal polarizations and colors in rule 6 are considered in the phase space (84).

4.4 Pair production amplitude

In the eikonal approximation, the gluon and quark pair only pick up a rotation in color phase space when they scatter off the color field of the nucleus [27]. In this way, the Wilson line propagator of eq. (21) with the corresponding color generators represents the effect of the interaction on the bare states. This is formulated using the eikonal scattering operator $\hat{\mathcal{S}}_E$ present in the matrix element for $q\bar{q}$ production⁴:

$${}_D \langle q_2 \bar{q}_3 | \hat{\mathcal{S}}_E - \mathbf{1} | g_1 \rangle_D = 2k_1^+ (2\pi) \delta(k_1^+ - k_2^+ - k_3^+) i \mathcal{M}_{g \rightarrow q\bar{q}} . \quad (94)$$

⁴ The $q\bar{q}$ state can exist in a color singlet or color octet configuration so that in the calculation of the cross section of this process, it would be necessary to add a color factor for both dressed states in eq. (94).

The scattering operator $\hat{\mathcal{S}}_E$ acts on the Fock states by color rotating each parton with a Wilson line defined along the trajectory of the parton through the target [27],

$$\hat{\mathcal{S}}_E \tilde{a}^\dagger(k^+, \mathbf{x}_\perp, \lambda, a) = U_A(\mathbf{x}_\perp)_{ba} \tilde{a}^\dagger(k^+, \mathbf{x}_\perp, \lambda, b) \hat{\mathcal{S}}_E, \quad (95)$$

$$\hat{\mathcal{S}}_E \tilde{b}^\dagger(k^+, \mathbf{x}_\perp, h, \alpha) = U_F(\mathbf{x}_\perp)_{\beta\alpha} \tilde{b}^\dagger(k^+, \mathbf{x}_\perp, h, \beta) \hat{\mathcal{S}}_E, \quad (96)$$

$$\hat{\mathcal{S}}_E \tilde{d}^\dagger(k^+, \mathbf{x}_\perp, h, \alpha) = [U_F^\dagger(\mathbf{x}_\perp)]_{\alpha\beta} \tilde{d}^\dagger(k^+, \mathbf{x}_\perp, h, \beta) \hat{\mathcal{S}}_E. \quad (97)$$

Here α (a) is the quark (gluon) color before the interaction and β (b) after. The $U_{F(A)}(\mathbf{x}_\perp)$ refers to the Wilson line at transverse coordinate \mathbf{x}_\perp in the fundamental (adjoint) representation. The Fock state vacuum is invariant under the action of the eikonal scattering operator: $\hat{\mathcal{S}}_E|0\rangle = |0\rangle$.

Hence, discarding the identity representing the non-interacting process, the matrix element in eq. (94) can be calculated with eqs. (95), (96), (97) and the normalization conditions in eq. (86) as

$$\begin{aligned} & {}_D \langle q_{2'} \bar{q}_{3'} | \hat{\mathcal{S}}_E | g_1 \rangle_D \\ &= \sqrt{Z_q}^2 \sqrt{Z_g} \int d^2 \mathbf{x}_{1\perp} e^{-i\mathbf{k}_{1\perp} \mathbf{x}_{1\perp}} \int d^2 \mathbf{x}'_{2\perp} e^{+i\mathbf{k}'_{2\perp} \mathbf{x}'_{2\perp}} \int d^2 \mathbf{x}'_{3\perp} e^{+i\mathbf{k}'_{3\perp} \mathbf{x}'_{3\perp}} \\ & \quad \times \left[{}_0 \langle \widetilde{q_{2'} \bar{q}_{3'}} | + \sum_{g_{1'}} \widetilde{{}_0 \langle g_{1'} | \tilde{\Psi}_{q_{2'} \bar{q}_{3'} \rightarrow g_{1'}}^\dagger} \right] | \hat{\mathcal{S}}_E | \left[|g_1\rangle_0 + \sum_{q_2 \bar{q}_3} \widetilde{\Psi}_{g_1 \rightarrow q_2 \bar{q}_3} | \widetilde{q_2 \bar{q}_3} \rangle_0 \right] \\ &= \int_{\mathbf{x}_{1\perp}} \int_{\mathbf{x}'_{2\perp}} \int_{\mathbf{x}'_{3\perp}} \left[\langle 0 | \tilde{d}_{3'} \tilde{b}_{2'} + \sum_{g_{1'}} \widetilde{\langle 0 | \tilde{a}_{1'} \tilde{\Psi}_{q_{2'} \bar{q}_{3'} \rightarrow g_{1'}}^\dagger} \right] | \hat{\mathcal{S}}_E | \left[\tilde{a}_1^\dagger | 0 \rangle + \sum_{q_2 \bar{q}_3} \widetilde{\Psi}_{g_1 \rightarrow q_2 \bar{q}_3} \tilde{b}_2^\dagger \tilde{d}_3^\dagger | 0 \rangle \right] \\ &= \int_{\mathbf{x}_{1\perp}} \int_{\mathbf{x}'_{2\perp}} \int_{\mathbf{x}'_{3\perp}} \left(\langle 0 | \tilde{d}_{3'} \tilde{b}_{2'} \hat{\mathcal{S}}_E \tilde{a}_1^\dagger | 0 \rangle + \sum_{q_2 \bar{q}_3} \widetilde{\Psi}_{g_1 \rightarrow q_2 \bar{q}_3} \langle 0 | \tilde{d}_{3'} \tilde{b}_{2'} \hat{\mathcal{S}}_E \tilde{b}_2^\dagger \tilde{d}_3^\dagger | 0 \rangle \right. \\ & \quad \left. + \sum_{g_{1'}} \widetilde{\Psi}_{q_{2'} \bar{q}_{3'} \rightarrow g_{1'}}^\dagger \langle 0 | \tilde{a}_{1'} \hat{\mathcal{S}}_E \tilde{a}_1^\dagger | 0 \rangle + \sum_{q_2 \bar{q}_3} \widetilde{|\Psi}_{g_1 \rightarrow q_2 \bar{q}_3}|^2 \langle 0 | \tilde{a}_{1'} \hat{\mathcal{S}}_E \tilde{b}_2^\dagger \tilde{d}_3^\dagger | 0 \rangle \right) \\ &= \int_{\mathbf{x}'_{2\perp}} \int_{\mathbf{x}'_{3\perp}} \sum_{q_2 \bar{q}_3} [U_F(\mathbf{x}_{2\perp})]_{\beta_2 \alpha_2} [U_F^\dagger(\mathbf{x}_{3\perp})]_{\alpha_3 \beta_3} \widetilde{\Psi}_{g_1 \rightarrow q_2 \bar{q}_3} \langle 0 | \tilde{d}_{3'} \tilde{b}_{2'} \tilde{b}_2^\dagger \tilde{d}_3^\dagger | 0 \rangle \\ & \quad + \int_{\mathbf{x}_{1\perp}} \sum_{g_{1'}} [U_A(\mathbf{x}_{1\perp})]_{ba} \widetilde{\Psi}_{q_{2'} \bar{q}_{3'} \rightarrow g_{1'}}^\dagger \langle 0 | \tilde{a}_{1'} \tilde{a}_1^\dagger | 0 \rangle. \end{aligned} \quad (98)$$

Here the renormalization coefficients $\sqrt{Z} \propto 1 + \mathcal{O}(g^2)$ as well as the states that are zero by orthogonality have been discarded. The integration over the transverse coordinates $\int_{\mathbf{x}_\perp} = d^2 \mathbf{x}_\perp e^{\pm i\mathbf{k}_\perp \mathbf{x}_\perp}$ is introduced to Fourier transform the dressed states

from momentum space to mixed space.

The vacuum expectation values in eq. (98) are calculated using the commutation relations in eq. (86) and the explicit expression of the phase space in eq. (84), where the polarization, helicity and color sums are left implicit:

$$\widetilde{\sum}_{q_2 \bar{q}_3} \langle 0 | \tilde{d}_3 \tilde{b}_2 \tilde{b}_2^\dagger \tilde{d}_3^\dagger | 0 \rangle \quad (99)$$

$$\begin{aligned} &= \int \frac{dk_2^+ \theta(k_2^+)}{2k_2^+ (2\pi)} \int \frac{dk_3^+ \theta(k_3^+)}{2k_3^+ (2\pi)} (2\pi) \delta(k_1^+ - k_2^+ - k_3^+) \int d^2 \mathbf{x}_{2\perp} \int d^2 \mathbf{x}_{3\perp} \\ &\quad \times (2k_2'^+) (2\pi) \delta(k_2'^+ - k_2^+) \delta^2(\mathbf{x}'_{2\perp} - \mathbf{x}_{2\perp}) \delta_{h_2' h_2} \delta_{\alpha_2' \beta_2} \langle 0 | \tilde{d}_3 \tilde{d}_3^\dagger | 0 \rangle \\ &= \int \frac{dk_2^+ \theta(k_2^+)}{2k_2^+ (2\pi)} \int \frac{dk_3^+ \theta(k_3^+)}{2k_3^+ (2\pi)} (2\pi) \delta(k_1^+ - k_2^+ - k_3^+) \int d^2 \mathbf{x}_{2\perp} \int d^2 \mathbf{x}_{3\perp} \\ &\quad \times (2k_2'^+) (2k_3'^+) (2\pi)^2 \delta(k_2'^+ - k_2^+) \delta(k_3'^+ - k_3^+) \delta^2(\mathbf{x}'_{2\perp} - \mathbf{x}_{2\perp}) \\ &\quad \times \delta^2(\mathbf{x}'_{3\perp} - \mathbf{x}_{3\perp}) \delta_{h_2' h_2} \delta_{h_3' h_3} \delta_{\alpha_2' \beta_2} \delta_{\alpha_3' \beta_3} \\ &= (2\pi) \delta(k_1^+ - k_2'^+ - k_3'^+) \delta_{h_2' h_2} \delta_{h_3' h_3} \delta_{\alpha_2' \beta_2} \delta_{\alpha_3' \beta_3} , \end{aligned}$$

$$\widetilde{\sum}_{g_1'} \langle 0 | \tilde{a}_1 \tilde{a}_1^\dagger | 0 \rangle \quad (100)$$

$$\begin{aligned} &= \int \frac{dk_1'^+ \theta(k_1'^+)}{2k_1'^+ (2\pi)} (2\pi) \delta(k_2'^+ + k_3'^+ - k_1'^+) \int d^2 \mathbf{x}'_{1\perp} \\ &\quad \times (2k_1'^+) (2\pi) \delta(k_1'^+ - k_1^+) \delta^{(2)}(\mathbf{x}'_{1\perp} - \mathbf{x}_{1\perp}) \delta_{\lambda' \lambda} \delta_{a' b} \\ &= (2\pi) \delta(k_2'^+ + k_3'^+ - k_1^+) \delta_{\lambda' \lambda} \delta_{a' b} . \end{aligned}$$

After performing the integration over the position coordinates and applying the Kronecker delta functions of color indices in eqs. (99) and (100), the color structure in eq. (98) results in

$$\begin{aligned} &[U_F(\mathbf{x}'_{2\perp})]_{\beta_2 \alpha_2} [U_F^\dagger(\mathbf{x}'_{3\perp})]_{\alpha_3 \beta_3} (t^a)_{\alpha_2 \alpha_3} \delta_{\alpha_2' \beta_2} \delta_{\alpha_3' \beta_3} + [U_A(\mathbf{x}_{1\perp})]_{ba} (t^{a'})_{\alpha_2' \alpha_3'}^\dagger \delta_{a' b} \\ &= [U_F(\mathbf{x}'_{2\perp})]_{\alpha_2' \alpha_2} (t^a)_{\alpha_2 \alpha_3} [U_F^\dagger(\mathbf{x}'_{3\perp})]_{\alpha_3 \alpha_3'} + (t^b)_{\alpha_3' \alpha_2'} [U_A(\mathbf{x}_{1\perp})]_{ba} \\ &= U_F(\mathbf{x}'_{2\perp}) t^a U_F^\dagger(\mathbf{x}'_{3\perp}) + t^b U_A^{ba}(\mathbf{x}_{1\perp}) . \end{aligned} \quad (101)$$

Here the color generators $(t^a)_{\alpha_2 \alpha_3}$ belong to the wave function (92).

The result in eq. (101) matches the color structure of the pair production amplitude (67) in the Lorenz gauge. At the cross section level, this color structure

contains a trace over the color indices due to the color factors of the dressed states.

The scattering amplitude (98) can be further solved using expressions (99), (100), (101) and the LCWF in eq. (93):

$$\begin{aligned}
& {}_D \langle q_2' \bar{q}_3' | \hat{\mathcal{S}}_E | g_1 \rangle_D \\
&= \int d^2 \mathbf{x}_{1\perp} e^{-i\mathbf{k}_{1\perp} \mathbf{x}_{1\perp}} \int d^2 \mathbf{x}'_{2\perp} e^{+i\mathbf{k}'_{2\perp} \mathbf{x}'_{2\perp}} \int d^2 \mathbf{x}'_{3\perp} e^{+i\mathbf{k}'_{3\perp} \mathbf{x}'_{3\perp}} \\
&\quad \times \left\{ (2\pi) \delta(k_1^+ - k_2'^+ - k_3'^+) \tilde{\Psi}_{g_1 \rightarrow q_2 \bar{q}_3} [U_F(\mathbf{x}'_{2\perp}) t^a U_F^\dagger(\mathbf{x}'_{3\perp})] \right. \\
&\quad \left. + (2\pi) \delta(k_2'^+ + k_3'^+ - k_1^+) \tilde{\Psi}_{q_2' \bar{q}_3' \rightarrow g_1'}^\dagger [t^b U_A^{ba}(\mathbf{x}_{1\perp})] \right\} \\
&= (2\pi) \delta(k_1^+ - k_2'^+ - k_3'^+) \int d^2 \mathbf{x}_{1\perp} e^{-i\mathbf{k}_{1\perp} \mathbf{x}_{1\perp}} \int d^2 \mathbf{x}'_{2\perp} e^{+i\mathbf{k}'_{2\perp} \mathbf{x}'_{2\perp}} \int d^2 \mathbf{x}'_{3\perp} e^{+i\mathbf{k}'_{3\perp} \mathbf{x}'_{3\perp}} \\
&\quad \times \left\{ -g \int \frac{d^2 \mathbf{k}_{2\perp}}{(2\pi)^2} \int \frac{d^2 \mathbf{k}_{3\perp}}{(2\pi)^2} e^{-i\mathbf{k}_{2\perp} \mathbf{x}'_{2\perp} - i\mathbf{k}_{3\perp} \mathbf{x}'_{3\perp}} (2\pi)^2 \delta^2(\mathbf{k}_{1\perp} - \mathbf{k}_{2\perp} - \mathbf{k}_{3\perp}) \right. \\
&\quad \times \frac{\bar{u}(k_2'^+, \mathbf{k}_{2\perp}) \left\{ \not{\epsilon}_\lambda [U_F(\mathbf{x}'_{2\perp}) t^a U_F^\dagger(\mathbf{x}'_{3\perp})] \right\} v(k_3'^+, \mathbf{k}_{3\perp})}{\left[\frac{\mathbf{k}_{1\perp}^2}{2k_1^+} - \frac{\mathbf{k}_{2\perp}^2 + m^2}{2k_2'^+} - \frac{\mathbf{k}_{3\perp}^2 + m^2}{2k_3'^+} \right]} \\
&\quad + g \int \frac{d^2 \mathbf{k}'_{1\perp}}{(2\pi)^2} e^{+i\mathbf{k}'_{1\perp} \mathbf{x}_{1\perp}} (2\pi)^2 \delta^2(\mathbf{k}'_{1\perp} - \mathbf{k}'_{2\perp} - \mathbf{k}'_{3\perp}) \\
&\quad \times \frac{\bar{u}(k_2'^+, \mathbf{k}'_{2\perp}) \left\{ \not{\epsilon}_\lambda [t^b U_A^{ba}(\mathbf{x}_{1\perp})] \right\} v(k_3'^+, \mathbf{k}'_{3\perp})}{\left[\frac{\mathbf{k}'_{1\perp}^2}{2k_1^+} - \frac{\mathbf{k}'_{2\perp}^2 + m^2}{2k_2'^+} - \frac{\mathbf{k}'_{3\perp}^2 + m^2}{2k_3'^+} \right]} \left. \right\} \\
&= (2\pi) \delta(k_1^+ - k_2'^+ - k_3'^+) \left(-g \int \frac{d^2 \mathbf{k}_{2\perp}}{(2\pi)^2} \int d^2 \mathbf{x}'_{2\perp} e^{+i(\mathbf{k}'_{2\perp} - \mathbf{k}_{2\perp}) \mathbf{x}'_{2\perp}} \right. \\
&\quad \times \int d^2 \mathbf{x}'_{3\perp} e^{+i(\mathbf{k}'_{3\perp} + \mathbf{k}_{2\perp}) \mathbf{x}'_{3\perp}} \frac{\bar{u}(k_2'^+, \mathbf{k}_{2\perp}) \left\{ \not{\epsilon}_\lambda [U_F(\mathbf{x}'_{2\perp}) t^a U_F^\dagger(\mathbf{x}'_{3\perp})] \right\} v(k_3'^+, -\mathbf{k}_{2\perp})}{\left[-\frac{\mathbf{k}_{2\perp}^2 + m^2}{2k_2'^+} - \frac{(-\mathbf{k}_{2\perp})^2 + m^2}{2k_3'^+} \right]} \\
&\quad \left. - \int d^2 \mathbf{x}_{1\perp} e^{+i(\mathbf{k}'_{2\perp} + \mathbf{k}'_{3\perp}) \mathbf{x}_{1\perp}} \frac{\bar{u}(k_2'^+, \mathbf{k}'_{2\perp}) \left\{ \not{\epsilon}_\lambda [t^b U_A^{ba}(\mathbf{x}_{1\perp})] \right\} v(k_3'^+, \mathbf{k}'_{3\perp})}{\left[\frac{(\mathbf{k}'_{2\perp} + \mathbf{k}'_{3\perp})^2}{2k_1^+} - \frac{\mathbf{k}'_{2\perp}^2 + m^2}{2k_2'^+} - \frac{\mathbf{k}'_{3\perp}^2 + m^2}{2k_3'^+} \right]} \right). \tag{102}
\end{aligned}$$

Here the orthogonality condition $\Psi^\dagger = -\Psi$ (88) has been applied and the integration

over $\mathbf{k}_{3\perp}$ and $\mathbf{k}'_{1\perp}$ has been solved with the delta functions. The momentum $\mathbf{k}_{1\perp}$ has been set to zero since the incoming gluon has zero transverse momentum before interacting with the CGC.

The result in eq. (102) allows to write eq. (94) as

$$\begin{aligned}
& 2k_1^+(2\pi)\delta(k_1^+ - k_2^+ - k_3^+)i\mathcal{M}_{g\rightarrow q'\bar{q}'} \\
&= (2\pi)\delta(k_1^+ - k_2^+ - k_3^+) \left(g \int \frac{d^2\mathbf{k}_{2\perp}}{(2\pi)^2} \int d^2\mathbf{x}'_{2\perp} e^{+i(\mathbf{k}'_{2\perp} - \mathbf{k}_{2\perp})\mathbf{x}'_{2\perp}} \right. \\
&\quad \times \int d^2\mathbf{x}'_{3\perp} e^{+i(\mathbf{k}'_{3\perp} + \mathbf{k}_{2\perp})\mathbf{x}'_{3\perp}} \frac{\bar{u}(k_2^+, \mathbf{k}_{2\perp}) \left\{ \not{\epsilon}_\lambda [U_F(\mathbf{x}'_{2\perp}) t^a U_F^\dagger(\mathbf{x}'_{3\perp})] \right\} v(k_3^+, -\mathbf{k}_{2\perp})}{\left[\frac{\mathbf{k}_{2\perp}^2 + m^2}{2k_2^+} + \frac{(-\mathbf{k}_{2\perp})^2 + m^2}{2k_3^+} \right]} \\
&\quad \left. + \int d^2\mathbf{x}_{1\perp} e^{+i(\mathbf{k}'_{2\perp} + \mathbf{k}'_{3\perp})\mathbf{x}_{1\perp}} \frac{\bar{u}(k_2^+, \mathbf{k}'_{2\perp}) \left\{ \not{\epsilon}_\lambda [t^b U_A^{ba}(\mathbf{x}_{1\perp})] \right\} v(k_3^+, \mathbf{k}'_{3\perp})}{\left[\frac{(\mathbf{k}'_{2\perp} + \mathbf{k}'_{3\perp})^2}{2k_1^+} - \frac{\mathbf{k}'_{2\perp}{}^2 + m^2}{2k_2^+} - \frac{\mathbf{k}'_{3\perp}{}^2 + m^2}{2k_3^+} \right]} \right), \tag{103}
\end{aligned}$$

where the quark pair production amplitude in light cone quantization can be read as⁵

$$\begin{aligned}
i\mathcal{M}_{g\rightarrow q'\bar{q}'}^{\text{LC}} &= g \int \frac{d^2\mathbf{k}_{2\perp}}{(2\pi)^2} \int d^2\mathbf{x}'_{2\perp} e^{+i(\mathbf{k}'_{2\perp} - \mathbf{k}_{2\perp})\mathbf{x}'_{2\perp}} \int d^2\mathbf{x}'_{3\perp} e^{+i(\mathbf{k}'_{3\perp} + \mathbf{k}_{2\perp})\mathbf{x}'_{3\perp}} \\
&\quad \times \frac{\bar{u}(k_2^+, \mathbf{k}_{2\perp}) \left\{ \not{\epsilon}_\lambda [U_F(\mathbf{x}'_{2\perp}) t^a U_F^\dagger(\mathbf{x}'_{3\perp})] \right\} v(k_3^+, -\mathbf{k}_{2\perp})}{2k_1^+ \left[\frac{\mathbf{k}_{2\perp}^2 + m^2}{2k_2^+} + \frac{(-\mathbf{k}_{2\perp})^2 + m^2}{2k_3^+} \right]} \\
&\quad + \int d^2\mathbf{x}_{1\perp} e^{+i(\mathbf{k}'_{2\perp} + \mathbf{k}'_{3\perp})\mathbf{x}_{1\perp}} \frac{\bar{u}(k_2^+, \mathbf{k}'_{2\perp}) \left\{ \not{\epsilon}_\lambda [t^b U_A^{ba}(\mathbf{x}_{1\perp})] \right\} v(k_3^+, \mathbf{k}'_{3\perp})}{2k_1^+ \left[\frac{(\mathbf{k}'_{2\perp} + \mathbf{k}'_{3\perp})^2}{2k_1^+} - \frac{\mathbf{k}'_{2\perp}{}^2 + m^2}{2k_2^+} - \frac{\mathbf{k}'_{3\perp}{}^2 + m^2}{2k_3^+} \right]}. \tag{104}
\end{aligned}$$

⁵ For a better comparison of the covariant and light-cone amplitude, the result has not been further simplified.

5 Comparison of the results

In this section, the following amplitudes obtained in covariant theory (67) and in LC quantization (104) are compared,

$$\begin{aligned}
i\mathcal{M}_{g \rightarrow q'\bar{q}'}^{\text{LC}} &= g \int \frac{d^2\mathbf{k}_{2\perp}}{(2\pi)^2} \int d^2\mathbf{x}'_{2\perp} e^{+i(\mathbf{k}'_{2\perp} - \mathbf{k}_{2\perp})\mathbf{x}'_{2\perp}} \int d^2\mathbf{x}'_{3\perp} e^{+i(\mathbf{k}'_{3\perp} + \mathbf{k}_{2\perp})\mathbf{x}'_{3\perp}} \\
&\quad \times \frac{\bar{u}(k_2^+, \mathbf{k}_{2\perp}) \left\{ \not{\epsilon}_\lambda [U_F(\mathbf{x}'_{2\perp}) t^a U_F^\dagger(\mathbf{x}'_{3\perp})] \right\} v(k_3^+, -\mathbf{k}_{2\perp})}{2k_1^+ \left[\frac{k_{2\perp}^2 + m^2}{2k_2^+} + \frac{(-\mathbf{k}_{2\perp})^2 + m^2}{2k_3^+} \right]} \\
&\quad + \int d^2\mathbf{x}_{1\perp} e^{+i(\mathbf{k}'_{2\perp} + \mathbf{k}'_{3\perp})\mathbf{x}_{1\perp}} \frac{\bar{u}(k_2^+, \mathbf{k}'_{2\perp}) \left\{ \not{\epsilon}_\lambda [t^b U_A^{ba}(\mathbf{x}_{1\perp})] \right\} v(k_3^+, \mathbf{k}'_{3\perp})}{2k_1^+ \left[\frac{(\mathbf{k}'_{2\perp} + \mathbf{k}'_{3\perp})^2}{2k_1^+} - \frac{k_{2\perp}^2 + m^2}{2k_2^+} - \frac{k_{3\perp}^2 + m^2}{2k_3^+} \right]}, \tag{105}
\end{aligned}$$

$$\begin{aligned}
\mathcal{M}_{g \rightarrow q\bar{q}}^{\text{cov}} &= g \int \frac{d^2\mathbf{k}_{1\perp}}{(2\pi)^2} \frac{d^2\mathbf{k}_\perp}{(2\pi)^2} \frac{g\rho_{p,a}(\mathbf{k}_{1\perp})}{k_{1\perp}^2} \int d^2\mathbf{x}_\perp d^2\mathbf{y}_\perp e^{i\mathbf{k}_\perp \mathbf{x}_\perp} e^{i(\mathbf{p}_\perp + \mathbf{q}_\perp - \mathbf{k}_\perp - \mathbf{k}_{1\perp})\mathbf{y}_\perp} \\
&\quad \times \bar{u}(q) \left\{ T_{q\bar{q}}(\mathbf{k}_{1\perp}, \mathbf{k}_\perp) [U_F(\mathbf{x}_\perp) t^a U_F^\dagger(\mathbf{y}_\perp)] + T_g(\mathbf{k}_{1\perp}) [t^b U_A^{ba}(\mathbf{x}_\perp)] \right\} v(p), \tag{106}
\end{aligned}$$

where

$$T_{q\bar{q}}(\mathbf{k}_{1\perp}, \mathbf{k}_\perp) \equiv \frac{\gamma^+(\not{q} - \not{k} + m)\gamma^-(\not{q} - \not{k} - \not{k}_1 + m)\gamma^+}{2p^+ [(\mathbf{q}_\perp - \mathbf{k}_\perp)^2 + m^2] + 2q^+ [(\mathbf{q}_\perp - \mathbf{k}_\perp - \mathbf{k}_{1\perp})^2 + m^2]}, \tag{107}$$

$$T_g(\mathbf{k}_{1\perp}) \equiv \frac{\mathcal{C}_L(p+q, \mathbf{k}_{1\perp})}{(p+q)^2}. \tag{108}$$

The first difference between both amplitudes is that the covariant amplitude (106) contains the incoming gluon density ρ_p integrated over the transverse momentum $\mathbf{k}_{1\perp}$, while in the LC amplitude (105) this factor is missing. This is because in covariant gauge, the proton is described as a classical field originated from the color current of valence sources in eq. (10). Then, the covariant amplitude includes a color charge density factor that when it is squared at the cross section level, it corresponds to the gluon distribution $xg(x, Q^2)$ of the proton presented in Figure 1 [28],

$$g \int \frac{d^2\mathbf{k}_{1\perp}}{(2\pi)^2} \frac{d^2\mathbf{k}'_{1\perp}}{(2\pi)^2} \frac{\langle \rho_{p,a}(k_{1\perp}) \rho_{p,a'}(k'_{1\perp}) \rangle}{k_{1\perp}^2} \rightarrow xg(x, Q^2), \tag{109}$$

where the expectation value $\langle \dots \rangle$ indicates the average of color sources [29].

In contrast, in light cone quantization the collision is described between a single gluon and a nucleus. To calculate the cross section of the proton-nucleus scattering, a factor corresponding to the distribution of gluons in the proton needs to be added, as it is already considered in covariant theory.

The gauge invariance can then be proved at the cross section level by taking the collinear approximation $\mathbf{k}_{1\perp} \rightarrow 0$ in the proton in covariant gauge. This limit is well defined since the second line in the covariant amplitude in eq. (106) goes to zero in the limit $\mathbf{k}_{1\perp} \rightarrow 0$ [16]. This can be proved by rewriting the terms in eqs. (107) and (108) as

$$\begin{aligned}
T_{q\bar{q}}(\mathbf{k}_{1\perp}, \mathbf{k}_{\perp}) &= \frac{\gamma^+(\not{q} - \not{k} + m)\gamma^-(\not{q} - \not{k} - \not{k}_1 + m)\gamma^+}{2p^+[(\mathbf{q}_{\perp} - \mathbf{k}_{\perp})^2 + m^2] + 2q^+[(\mathbf{q}_{\perp} - \mathbf{k}_{\perp} - \mathbf{k}_{1\perp})^2 + m^2]}, \quad (110) \\
&\stackrel{\text{K}_{1\perp} \rightarrow 0}{=} \frac{(\not{q}_{\perp} - \not{k}_{\perp} + m)\gamma^+\gamma^-\gamma^+(\not{q}_{\perp} - \not{k}_{\perp} + m)}{2p^+[(\mathbf{q}_{\perp} - \mathbf{k}_{\perp})^2 + m^2] + 2q^+[(\mathbf{q}_{\perp} - \mathbf{k}_{\perp})^2 + m^2]}, \\
&= \frac{(\not{q}_{\perp} - \not{k}_{\perp} + m)2\gamma^+(\not{q}_{\perp} - \not{k}_{\perp} + m)}{2[(\mathbf{q}_{\perp} - \mathbf{k}_{\perp})^2 + m^2](q^+ + p^+)}, \\
&= \frac{2(\not{q}_{\perp} - \not{k}_{\perp} + m)(-(\not{q}_{\perp} - \not{k}_{\perp}) + m)\gamma^+}{2[(\mathbf{q}_{\perp} - \mathbf{k}_{\perp})^2 + m^2](q^+ + p^+)}, \\
&= \frac{-[(\not{q}_{\perp} - \not{k}_{\perp})^2 - m^2]\gamma^+}{[(\mathbf{q}_{\perp} - \mathbf{k}_{\perp})^2 + m^2](q^+ + p^+)}, \\
&= \frac{-[-(\mathbf{q}_{\perp} - \mathbf{k}_{\perp})^2 - m^2]\gamma^+}{[(\mathbf{q}_{\perp} - \mathbf{k}_{\perp})^2 + m^2](q^+ + p^+)}, \\
&= \frac{\gamma^+}{(q^+ + p^+)}, \\
T_g(\mathbf{k}_{1\perp}, \mathbf{k}_{\perp}) &= \left[\frac{\mathcal{C}'_U(p+q, \mathbf{k}_{1\perp})}{(p+q)^2} - \frac{\gamma^+}{p^+ + q^+} \right]_{\mathbf{k}_{1\perp} \rightarrow 0} \stackrel{\text{K}_{1\perp} \rightarrow 0}{=} -\frac{\gamma^+}{(q^+ + p^+)}. \quad (111)
\end{aligned}$$

Here the identities $\gamma^+\gamma^-\gamma^+ = 2\gamma^+$, $(\gamma^+)^2 = (\gamma^-)^2 = 0$ and $\{\gamma^i, \gamma^j\} = -2\delta^{ij}$ have been used in eq. (110). Equation (111) contains the Lipatov term in eq. (108) rewritten using eq. (63). The $C_U(p+q, \mathbf{k}_{1\perp})$ coefficient defined in eq. (19) is zero in the collinear limit. Thus, the curly bracket in the covariant amplitude (106) becomes

$$\frac{\bar{u}(q)\gamma^+[U_F(\mathbf{x}_{\perp})t^a U_F^{\dagger}(\mathbf{y}_{\perp})]v(p)}{p^+ + q^+} - \frac{\gamma^+\bar{u}(q)[t^b U_A^{ba}(\mathbf{x}_{\perp})]v(p)}{p^+ + q^+}. \quad (112)$$

Since this expression does not depend on \mathbf{k}_{\perp} anymore, the integration over \mathbf{k}_{\perp} in eq.

(106) produces a $\delta(\mathbf{x}_\perp - \mathbf{y}_\perp)$. Therefore, the $U_F(\mathbf{x}_\perp)t^a U_F^\dagger(\mathbf{y}_\perp)$ factor can be replaced by $t^b U_A^{ba}(\mathbf{x}_\perp)$ using eq. (56) and the cancellation between the two terms is proved. Then, the amplitude factorizes as

$$\mathcal{M}_{\text{cov}} \Big|_{\mathbf{k}_{1\perp} \rightarrow 0} = \mathbf{A} \cdot \mathbf{k}_{1\perp} , \quad (113)$$

where the vector \mathbf{A} contains spinors and Dirac matrices [29]. Therefore, when the amplitude in eq. (113) is squared, it cancels a factor $k_{1\perp}^2$ in the denominator of the unintegrated gluon distribution in eq. (106) and the gluon distribution in eq. (109) is well defined in the collinear limit.

Another difference between the amplitudes (105) and (106) is the Dirac structure. In the LC amplitude (105) the transverse polarization vector ϵ_λ of the gluon is explicitly written in the quark-gluon vertex in eq. (89), while in covariant theory, the polarization of the incoming gluon is added at the cross section level. However, the Dirac structure $T_{q\bar{q}}$ in eq. (107) between the two Dirac spinors $\bar{u}(q)$ and $v(p)$ can be rewritten using the completeness relation of the spinors [23]

$$\sum_h u(k, h)\bar{u}(k, h) = \not{k} + m , \quad (114)$$

$$\sum_h v(k, h)\bar{v}(k, h) = \not{k} - m , \quad (115)$$

and the following orthogonality relations

$$\bar{u}(k^+, h)\gamma^+ u(q^+, s) = \bar{v}(k^+, h)\gamma^+ v(q^+, s) = \sqrt{2k^+}\sqrt{2q^+}\delta_{h,s} , \quad (116)$$

$$\bar{u}(k^+, h)\gamma^+ v(q^+, s) = \bar{v}(k^+, h)\gamma^+ u(q^+, s) = \sqrt{2k^+}\sqrt{2q^+}\delta_{h,-s} , \quad (117)$$

$$\begin{aligned}
& \bar{u}(q)T_{q\bar{q}}(\mathbf{k}_{1\perp},\mathbf{k}_{\perp})v(p) \\
&= \frac{\bar{u}(q)\gamma^+(\not{q}-\not{k}+m)\gamma^-(\not{q}-\not{k}-\not{k}_1+m)\gamma^+v(p)}{2p^+[(\mathbf{q}_{\perp}-\mathbf{k}_{\perp})^2+m^2]+2q^+[(\mathbf{q}_{\perp}-\mathbf{k}_{\perp}-\mathbf{k}_{1\perp})^2+m^2]} \\
&= -\frac{\bar{u}(q)\gamma^+(\not{q}-\not{k}+m)\gamma^-(-\not{q}+\not{k}+\not{k}_1-m)\gamma^+v(p)}{2p^+2q^+[\frac{(\mathbf{q}_{\perp}-\mathbf{k})^2+m^2}{2q^+}]+2q^+2(q^+-k_1^+)[\frac{(\mathbf{q}_{\perp}-\mathbf{k}_{\perp}-\mathbf{k}_{1\perp})^2+m^2}{2(q^+-k_1^+)}]} \\
&= -\frac{\bar{u}(q)\gamma^+u(q-k)\bar{u}(q-k)\gamma^-v(k+k_1-q)\bar{v}(k+k_1-q)\gamma^+v(p)}{4p^+q^+(q^- - k^-) + 4q^+(-p^+)(q^- - k^- - k_1^-)} \tag{118} \\
&= -\frac{(2\sqrt{q^+}\sqrt{q^+ - k^+})(2p^+)\bar{u}(q-k)\gamma^-v(k+k_1-q)}{4p^+q^+(q^- - k^-) + 4q^+(-p^+)(q^- - k^- - k_1^-)} \\
&= -\frac{\bar{u}(q-k)\gamma^-v(k+k_1-q)}{(q^- - k^-) + (-q^- + k^- + k_1^-)}.
\end{aligned}$$

Here it has been set $k^+ = 0$ since the nucleus is moving in the x^- -direction. The momentum conservation $k + k_1 - q = p$ has also been used.

The color current of the proton in eq. (10) has only a (+)-component, imposed by the $\delta^{\nu+}$, because the proton is moving in the (+)-axis in the LC. Since this current only produces a (+)-component of the proton gauge field A_p^+ in eq. (11), the only component of the polarization vector that would be relevant is ϵ^+ . If the latter were considered in the calculations of the covariant amplitude, it would have been contracted with a γ^- factor, which is the factor obtained in eq. (118). Furthermore, in eq. (118) the momenta of the spinors as well as the energy denominator, corresponds to the intermediate propagator before the interaction with the shockwave. In this way, the expression is equivalent, except for a factor of $2k_1^+$, to the corresponding term in the LC amplitude (105), where the intermediate momenta can be identified as $k_2 = q - k$ and $k_3 = -q + k + k_1$.

The Dirac structure in eq. (108) contains the Lipatov vertex $C_L^\mu(p+q, \mathbf{k}_{1\perp})$ defined in eq. (64). It has not been obtained a clear expression of the above Lipatov vertex compatible with the polarization vector in the numerator of the LC amplitude (105).

However, the energy denominator in eq. (108) can be rewritten as

$$\begin{aligned}
(p+q)^2 &= 2(p^+ + q^+)(p^- + q^-) - (\mathbf{p}_\perp + \mathbf{q}_\perp)^2 \\
&= 2k_1'^+ \left[\frac{\mathbf{p}_\perp^2 + m^2}{p^+} + \frac{\mathbf{q}_\perp^2 + m^2}{q^+} \right] - \mathbf{k}_{1\perp}'^2 \\
&= 2k_1'^+ \left[\frac{\mathbf{p}_\perp^2 + m^2}{p^+} + \frac{\mathbf{q}_\perp^2 + m^2}{q^+} - \frac{\mathbf{k}_{1\perp}'^2}{2k_1'^+} \right],
\end{aligned} \tag{119}$$

where the momentum conservation $\mathbf{p}_\perp + \mathbf{q}_\perp = \mathbf{k}'_{1\perp}$ has been applied. By identifying $\mathbf{k}'_{1\perp} = \mathbf{k}'_{2\perp} + \mathbf{k}'_{3\perp}$, $\mathbf{p}_\perp = \mathbf{k}'_{2\perp}$ and $\mathbf{q}_\perp = \mathbf{k}'_{3\perp}$, the expression in eq. (119) has the same structure as the energy denominator in the second term of eq. (105).

Although the modulus squared of the amplitudes is taken to calculate the cross section, the LC amplitude (105) is imaginary whereas the covariant amplitude (106) is real. The last difference observed between the two theories is that in light cone quantization, all the particles are on-shell but the $(-)$ -component of the momentum is not conserved at the vertices of the diagrams. In covariant theory, particles are off-shell, but the $(-)$ -component of the momentum is conserved. Thus, at the end, the calculation made in the two theories is equivalent.

6 Conclusions

The aim of this thesis was getting the probability amplitude of a gluon splitting into a quark-antiquark pair in proton-nucleus collisions at high-energy.

The first result is obtained in the Lorenz gauge, showed in eq. (67) in section 3, where the proton-nucleus collision is described as an interaction between classical color fields originated from color sources, following [3, 16]. The result is structured into two terms representing the two possible time-ordered interactions in the light cone. The first one corresponds to the splitting of a gluon into a $q\bar{q}$ -pair and the subsequent interaction with the CGC in the nucleus. The second one describes the multiple scatterings of a gluon off the saturated gluonic region before its splitting. In both cases, the interaction is represented in the eikonal approximation by a color rotation through Wilson Lines in the fundamental $U_F(\mathbf{x}_\perp)$ and adjoint $U_A(\mathbf{x}_\perp)$ representations.

In section 4 the production amplitude describing the same process is calculated in eq. (104) using light cone quantization. In this formalism, the Fock state basis in terms of the bare states is used to expand the initial gluon and final quark-antiquark dressed states. Similarly as the covariant amplitude (67), the interaction of each parton with the CGC is represented by Wilson Lines in the LC amplitude (104). In this calculation, the polarization of the incoming gluon is explicitly considered, in contrast with the calculation made in covariant theory.

In section 5, a comparison of both results is made and the Dirac structure as well as the energy denominators in the covariant amplitude (67) are rewritten to show their equivalence with the LC amplitude (104).

To completely prove the gauge invariance of the results, it is necessary to complete the cross section calculation by squaring the amplitudes in the collinear limit $\mathbf{k}_{1\perp} \rightarrow 0$ for the gluon momentum in the proton. Before taking this approximation, the amplitudes in the LCPT and covariant theory contain factors that can not be compared, such as the unintegrated gluon distribution (109) or the Lipatov factor (108).

The result of this work can be used to calculate the cross section of pair production

that can be compared to experimental data in proton-nucleus collisions at the LHC. The aim is to better understand the structure of the proton at the high-energy regime.

References

- [1] F. Gelis. “Color Glass Condensate and Glasma”. In: *Int. J. Mod. Phys. A* 28 (2013), p. 1330001. DOI: 10.1142/S0217751X13300019. arXiv: 1211.3327 [hep-ph].
- [2] S. Bailey et al. “Parton distributions from LHC, HERA, Tevatron and fixed target data: MSHT20 PDFs”. In: *The European Physical Journal C* 81.4 (2021). DOI: 10.1140/epjc/s10052-021-09057-0. URL: <https://doi.org/10.1140/epjc/s10052-021-09057-0>.
- [3] J. P. Blaizot, F. Gelis, and R. Venugopalan. “High-energy pA collisions in the color glass condensate approach. 1. Gluon production and the Cronin effect”. In: *Nucl. Phys. A* 743 (2004), pp. 13–56. DOI: 10.1016/j.nuclphysa.2004.07.005. arXiv: hep-ph/0402256.
- [4] P. A. M. Dirac. “Forms of Relativistic Dynamics”. In: *Rev. Mod. Phys.* 21 (3 1949), pp. 392–399. DOI: 10.1103/RevModPhys.21.392. URL: <https://link.aps.org/doi/10.1103/RevModPhys.21.392>.
- [5] R. Venugopalan. “Introduction to light cone field theory and high energy scattering”. In: *Hadrons in Dense Matter and Hadrosynthesis*. Springer Berlin Heidelberg, pp. 89–112. DOI: 10.1007/bfb0107312. URL: <https://doi.org/10.1007/bfb0107312>.
- [6] T. Lappi. *Lecture notes in High Energy Scattering in QCD(Advanced Course)*. University of Jyväskylä, 2023.
- [7] A. Accardi et al. “Electron Ion Collider: The Next QCD Frontier: Understanding the glue that binds us all”. In: *Eur. Phys. J. A* 52.9 (2016). Ed. by A. Deshpande, Z. E. Meziani, and J. W. Qiu, p. 268. DOI: 10.1140/epja/i2016-16268-9. arXiv: 1212.1701 [nucl-ex].
- [8] I. I. Balitsky and L. N. Lipatov. “The Pomernanchuk Singularity in Quantum Chromodynamics”. In: *Sov. J. Nucl. Phys.* 28 (1978), pp. 822–829.

- [9] E. A. Kuraev, L. N. Lipatov, and V. S. Fadin. “The Pomeron Singularity in Nonabelian Gauge Theories”. In: *Sov. Phys. JETP* 45 (1977), pp. 199–204.
- [10] M. Froissart. “Asymptotic behavior and subtractions in the Mandelstam representation”. In: *Phys. Rev.* 123 (1961), pp. 1053–1057. DOI: 10.1103/PhysRev.123.1053.
- [11] F. Gelis et al. “The Color Glass Condensate”. In: *Ann. Rev. Nucl. Part. Sci.* 60 (2010), pp. 463–489. DOI: 10.1146/annurev.nucl.010909.083629. arXiv: 1002.0333 [hep-ph].
- [12] E. Iancu and R. Venugopalan. “The Color glass condensate and high-energy scattering in QCD”. In: *Quark-gluon plasma 4*. Ed. by R. C. Hwa and X.-N. Wang. Mar. 2003, pp. 249–3363. DOI: 10.1142/9789812795533_0005. arXiv: hep-ph/0303204.
- [13] H. Weigert. “Evolution at small $x(bj)$: The Color glass condensate”. In: *Prog. Part. Nucl. Phys.* 55 (2005), pp. 461–565. DOI: 10.1016/j.pnpnp.2005.01.029. arXiv: hep-ph/0501087.
- [14] Y. V. Kovchegov and E. Levin. *Quantum Chromodynamics at High Energy*. Cambridge Monographs on Particle Physics, Nuclear Physics and Cosmology. Cambridge University Press, 2012. DOI: 10.1017/CB09781139022187.
- [15] Z.-B. Kang, Y.-Q. Ma, and R. Venugopalan. “Quarkonium production in high energy proton-nucleus collisions: CGC meets NRQCD”. In: *JHEP* 01 (2014), p. 056. DOI: 10.1007/JHEP01(2014)056. arXiv: 1309.7337 [hep-ph].
- [16] J. P. Blaizot, F. Gelis, and R. Venugopalan. “High-energy pA collisions in the color glass condensate approach. 2. Quark production”. In: *Nucl. Phys. A* 743 (2004), pp. 57–91. DOI: 10.1016/j.nuclphysa.2004.07.006. arXiv: hep-ph/0402257.
- [17] F. Gelis and Y. Mehtar-Tani. “Gluon propagation inside a high-energy nucleus”. In: *Phys. Rev. D* 73 (2006), p. 034019. DOI: 10.1103/PhysRevD.73.034019. arXiv: hep-ph/0512079.
- [18] A. J. Baltz et al. “Coulomb corrections to $e^+ e^-$ production in ultrarelativistic nuclear collisions”. In: *Nucl. Phys. A* 695 (2001), pp. 395–429. DOI: 10.1016/S0375-9474(01)01109-5. arXiv: nucl-th/0101024.

- [19] L. Lipatov. “Reggeization of the vector meson and the vacuum singularity in nonabelian gauge theories”. In: *Yad. Fiz.;(USSR)* 23.3 (1976).
- [20] V. Del Duca. “An introduction to the perturbative QCD pomeron and to jet physics at large rapidities”. In: (Feb. 1995). arXiv: hep-ph/9503226.
- [21] J. D. Bjorken, J. B. Kogut, and D. E. Soper. “Quantum Electrodynamics at Infinite Momentum: Scattering from an External Field”. In: *Phys. Rev. D* 3 (1971), p. 1382. DOI: 10.1103/PhysRevD.3.1382.
- [22] S. J. Brodsky, H.-C. Pauli, and S. S. Pinsky. “Quantum chromodynamics and other field theories on the light cone”. In: *Phys. Rept.* 301 (1998), pp. 299–486. DOI: 10.1016/S0370-1573(97)00089-6. arXiv: hep-ph/9705477.
- [23] G. Beuf. “Dipole factorization for DIS at NLO: Loop correction to the $\gamma_{T,L}^* \rightarrow q\bar{q}$ light-front wave functions”. In: *Phys. Rev. D* 94.5 (2016), p. 054016. DOI: 10.1103/PhysRevD.94.054016. arXiv: 1606.00777 [hep-ph].
- [24] T. Lappi and R. Paatelainen. “The one loop gluon emission light cone wave function”. In: *Annals of Physics* 379 (2017), pp. 34–66. ISSN: 0003-4916. DOI: <https://doi.org/10.1016/j.aop.2017.02.002>. URL: <https://www.sciencedirect.com/science/article/pii/S0003491617300507>.
- [25] G. Beuf, T. Lappi, and R. Paatelainen. “Massive quarks in NLO dipole factorization for DIS: Longitudinal photon”. In: *Phys. Rev. D* 104.5 (2021), p. 056032. DOI: 10.1103/PhysRevD.104.056032. arXiv: 2103.14549 [hep-ph].
- [26] G. P. Lepage and S. J. Brodsky. “Exclusive Processes in Perturbative Quantum Chromodynamics”. In: *Phys. Rev. D* 22 (1980), p. 2157. DOI: 10.1103/PhysRevD.22.2157.
- [27] E. Iancu et al. “Gluon dipole factorisation for diffractive dijets”. In: (July 2022). arXiv: 2207.06268 [hep-ph].
- [28] H. Fujii, F. Gelis, and R. Venugopalan. “Quantitative study of the violation of k-perpendicular-factorization in hadroproduction of quarks at collider energies”. In: *Phys. Rev. Lett.* 95 (2005), p. 162002. DOI: 10.1103/PhysRevLett.95.162002. arXiv: hep-ph/0504047.
- [29] H. Fujii and K. Watanabe. “Heavy quark pair production in high energy pA collisions: Quarkonium”. In: *Nucl. Phys. A* 915 (2013), pp. 1–23. DOI: 10.1016/j.nuclphysa.2013.06.011. arXiv: 1304.2221 [hep-ph].